



HAL
open science

Coalescence in fully asynchronous elementary cellular automata

Jordina Francès de Mas

► **To cite this version:**

Jordina Francès de Mas. Coalescence in fully asynchronous elementary cellular automata. Cellular Automata and Lattice Gases [nlin.CG]. 2017. hal-01627454

HAL Id: hal-01627454

<https://inria.hal.science/hal-01627454>

Submitted on 1 Nov 2017

HAL is a multi-disciplinary open access archive for the deposit and dissemination of scientific research documents, whether they are published or not. The documents may come from teaching and research institutions in France or abroad, or from public or private research centers.

L'archive ouverte pluridisciplinaire **HAL**, est destinée au dépôt et à la diffusion de documents scientifiques de niveau recherche, publiés ou non, émanant des établissements d'enseignement et de recherche français ou étrangers, des laboratoires publics ou privés.



UNIVERSITÉ
DE LORRAINE



Coalescence in fully asynchronous elementary cellular automata

Jordina Francès de Mas

MSc in Dependable Software Systems (DESEM)

1st year

supervised by

Nazim Fatès¹ & Irène Marcovici²

¹ LORIA, INRIA – nazim.fates@loria.fr

² IECL, Université de Lorraine – irene.marcovici@univ-lorraine.fr

October 31, 2017

Abstract

Cellular automata (CA) are discrete mathematical systems formed by a set of cells arranged in a regular fashion. Each of these cells is in a particular state and evolves according to a local rule depending on the state of the cells in its neighbourhood. In spite of their apparent simplicity, these dynamical systems are able to display a complex emerging behaviour, and the macroscopic structures they produce are not always predictable despite complete local knowledge.

While studying the robustness of CA to the introduction of asynchronism in their updating scheme, a phenomenon called coalescence was observed for the first time: for some asynchronous CA, the application of the same local rule on any two different initial conditions following the same sequence of updates quickly led to the same non-trivial configuration. Afterwards, it was experimentally found that some CA would always coalesce whilst others would never coalesce, and that some of them exhibit a phase transition between a coalescing and non-coalescing behaviour.

However, a formal explanation of non-trivial rapid coalescence has yet to be found, and this is the purpose of this project, where we try to characterise and explain this phenomenon both qualitatively and analytically. In particular, we analytically study trivial coalescence, find lower bounds for the coalescence time of ECA 154 and ECA 62, and give some first steps towards finding their upper bounds in order to prove that they have, respectively, quadratic and linear coalescence time.

Contents

1	Introduction	2
1.1	Main properties and history of CA	2
1.2	Asynchronism and coalescence	3
2	Definitions and notation	6
2.1	CA and ECA	6
2.2	Updating schemes and fixed points	9
2.3	ECA properties	11
2.3.1	Symmetries and equivalence classes	11
2.3.2	Linearity, affinity, quiescence, homogeneity and universality	12
3	Precedings	17
4	Visualisation and qualitative exploration	18
5	Definitions of coalescence behaviours	20
6	Analytical tools	25
7	Analytical study	26
7.1	Fixed points and homogenising ECA	26
7.2	Study of trivial coalescence	28
7.3	Quadratic coalescence study	29
7.3.1	Local behaviour analysis	30
7.3.2	Global behaviour analysis	30
7.3.3	Mathematical analysis	32
7.4	Linear coalescence study	36
8	Conclusion	38
A	Taxonomy table	44

1 Introduction

1.1 Main properties and history of CA

Cellular automata (CA) are discrete mathematical systems formed by a set of cells arranged in a regular fashion. Each of these cells is in a particular state and evolves according to a local rule depending on the state of the cells in its neighbourhood. Despite of their apparent simplicity — they are a set of cells updating their state in discrete time by following simple local rules—, these dynamical systems are able to display complex emerging behaviour. As Epstein wrote, “even perfect knowledge of individual decision rules does not always allow us to predict macroscopic structure. We get macro-surprises despite complete micro-knowledge” [12].

Example 1.1. The one-dimensional binary cellular automaton which simultaneously updates every cell with the sum modulo 2 of its right and left neighbours, known as ECA 90 (see page 6 for a formal definition of Elementary Cellular Automata), initialised with a single cell in state one generates the Sierpiński triangle, a very famous fractal structure (see Figure 1).

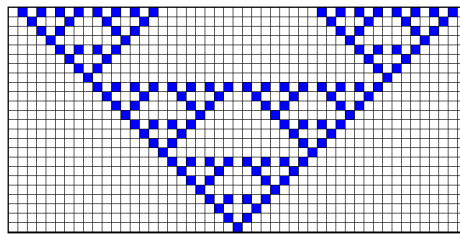


Figure 1: Space-time diagram (see page 7) showing the evolution, from bottom to top, of ECA 90, where each row represents the ECA state at consecutive times. The initial configuration is the bottom row, where there is a single cell in state one (blue), and the rest are in state zero (white). At each time step, each cell is simultaneously updated with the sum modulo 2 of its right and left neighbours, and the resulting configuration is plot on top of its predecessor.

CA were introduced by von Neumann in the 1950s when he was studying the problem of self-replicating systems [44] and, following a suggestion of his colleague Stanislaw Ulam, he focused on the study of a two-dimensional discrete model [45]. The particular CA he worked with was rather complicated, with 29 possible states for each cell, but prospective studies would show that even the simplest kind of CA are capable of modelling numerous complex systems, such as those with many interacting elements in biology [20] (e.g. biological cells [1], swarming phenomenon [9], pattern formation [10, 22, 30]), physics (e.g. ideal gases and fluids [43]), chemistry (e.g. anodisation process [3]), economics (e.g. financial market [2]), sociology and ecology [11, 35, 47], among others. These results show that CA are not merely abstract systems, but can directly correspond to natural processes.

Example 1.2. Kusch and Markus and Coombes showed that the pigmentation patterns on mollusc’s shells could be generated by CA models [8, 22]. More recently, Manukyan et al. demonstrated that

the colour pattern of the ocellated lizards' skin scales can be modeled by a cellular automaton [30] (see Figure 2).

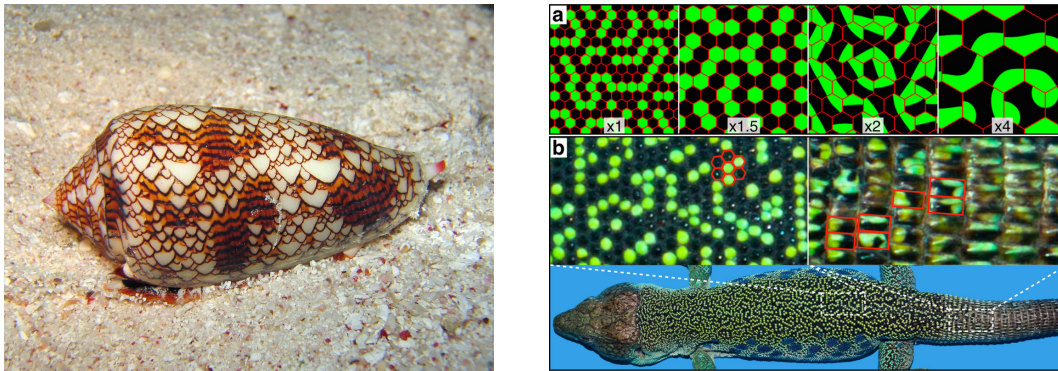


Figure 2: *Conus textile* shell exhibiting a pattern that can be identified with ECA 30 (left, reprinted from [8]), and ocellated lizard scales skin exhibiting a pattern that can be identified with a quasi-hexagonal probabilistic CA (right, reprinted from [30]).

In the 1960s, the computation capabilities of CA were noticed and started to be formally studied. CA, like Turing machines, can be fully specified in mathematical terms and implemented in physical structures, but the main difference is that they perform computations in a *parallel*, distributed fashion. It was proven that some CA can emulate a universal Turing machine, and therefore compute, according to Church–Turing thesis, anything computable.

Example 1.3. The most popular CA is probably Conway’s *Game of Life* [19]. It is a two-dimensional CA which exhibits a range of complex and interesting behaviour, and it is one of the simplest computational models ever proved to be Turing-complete [4]. The simplest known model capable of universal computation is a one-dimensional binary CA known as ECA 110, the behaviour of which is on the boundary between stability and chaos [7]. These findings suggest that, surprisingly enough, naturally occurring physical systems may also be capable of universality! However, note that other factors such as noise and asynchronism may be present in real systems, and these factors can alter the universality capabilities of the system (see Remark on page 15).

In the 1980s, Wolfram started to work on cellular automata and published several papers [31, 43, 48, 49] that led to a rapid increase of scientific interest in the field. He extensively explored one-dimensional CA, and in 2002 he published a 1280-page book summarising his work, findings and ideas, arguing that CA have significance for all disciplines of science, and providing the groundwork for further research [50].

1.2 Asynchronism and coalescence

In their original definition, CA cells are all updated in parallel at each time step, that is, synchronously. However, it could be argued that other updating methods better model real systems where asynchronism, noise and errors may be present. It was observed that even a small change in

this CA feature could strongly modify their behaviour and properties (see e.g. [16]). Surprisingly, some CA behave the same if their cells are updated in a synchronous or an asynchronous manner (we call these to be “robust” to asynchronism), but the behaviour of some other CA drastically changes when different updating styles are used. The systematic study of these kind of perturbations showed that some previously observed behaviours and properties were, in fact, artifacts of a synchronous updating and the use of a regular disposition of the cells [14]. This gave rise to the study of other classes of CA, namely asynchronous CA, probabilistic CA, and CA with alternative cell shapes and arrangements.

While studying the “robustness” of ECA to the introduction of asynchronism in their updating scheme, Fatès and Morvan observed one of these aforementioned “macro-surprises”: for some asynchronous ECA, the application of the same local rule on any two different initial conditions following the same sequence of updates quickly led to the exact same configuration [16] (see Figures 3 and 4). This surprising phenomenon is called *coalescence* and it was experimentally studied by Rouquier and Morvan, who showed that some ECA would always coalesce whilst others would never coalesce, and that some of them exhibit a phase transition between a coalescing and non-coalescing behaviour [38–42]. However, a formal explanation of non-trivial rapid coalescence has yet to be found, and this is the purpose of this project, where we try to characterise and explain this phenomenon both qualitatively and analytically.

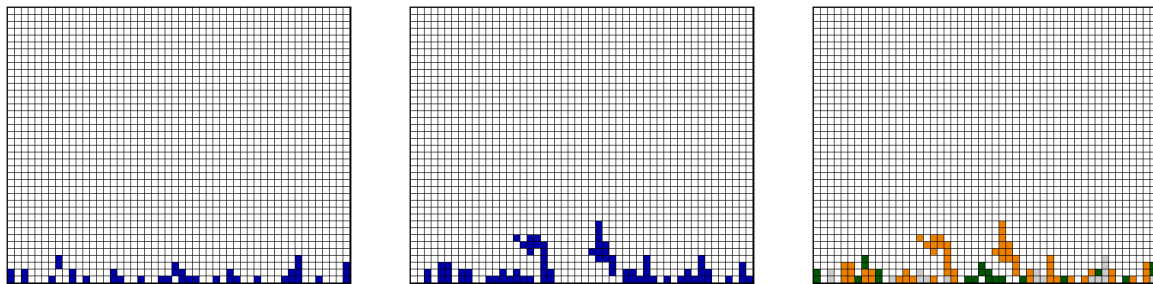


Figure 3: Evolution, from bottom to top, of ECA 2 under fully asynchronous updating (see Section 2.2) and starting from two different initial configurations (left and centre). Diagram with the superimposition of both CA showing their differences in green and orange (right).

It is quite obvious that a CA which, given any initial configuration and following any sequence of updates, always reaches the same configuration (typically, a fixed point) after some time will be coalescent. For example, ECA 0 (where any input configuration becomes zero) and ECA 255 (where any input configuration becomes one). This phenomenon can thus be called trivial coalescence (see Figure 3). On the other hand, non-trivial coalescence has also been observed [16, 42] (see Figure 4), and so this suggests that the asymptotic behaviour of some CA could be completely independent of the initial configuration but strongly dependent on the sequence of updates.

Remember that CA are deterministic in the sense that starting from the same initial configuration and updating the same cells in the same order will lead to the exact same result. However, their global behaviour may be very complex, even chaotic, and difficult to predict, so we would not expect them to synchronise. Therefore, it is puzzling to see that an apparent non-trivial configuration (like

the evolution of ECA 46 that we can see in Figure 4) is always reached from any initial condition if the same updating sequence is followed, especially when this happens very quickly! Thinking of CA as complex systems, many questions about this unexpected synchronisation phenomenon arise: will two complex systems be able to synchronise? If so, how long will it take? Will this synchronisation be independent or dependent on the initial configuration? Will the order in which the cells are updated matter? In how many different states is a complex system able to coalesce? How robust is this property? The study of these kind of questions can help us understand and build complex systems robust to some perturbations or with a specific global behaviour independent of its initial state.

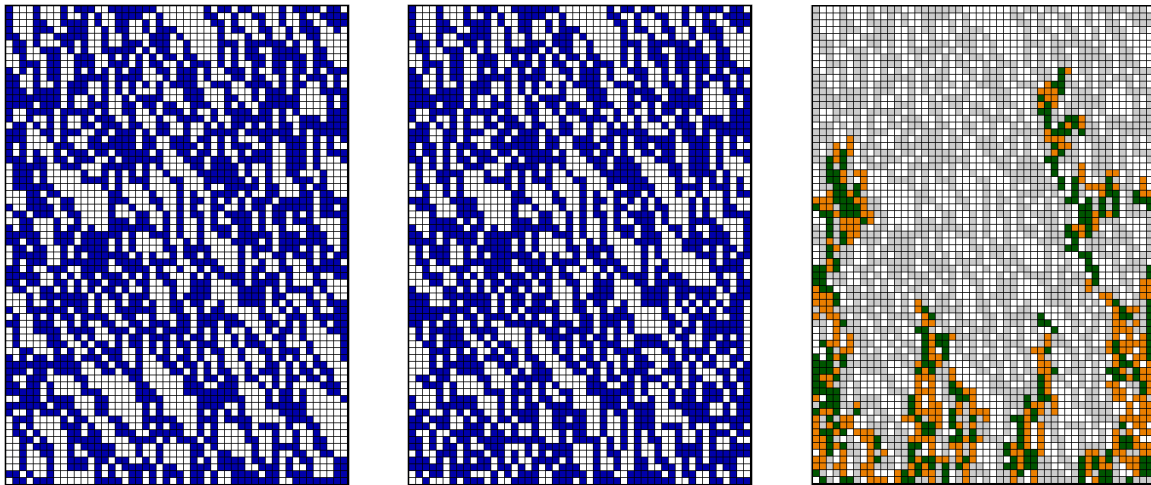


Figure 4: Evolution, from bottom to top, of ECA 46 with periodic boundary conditions (see page 8) following the same partially asynchronous updating sequence (see Section 2.2) and starting from two different initial configurations (left and centre). Diagram with the superimposition of both CA showing their differences in green and orange and their agreement in white and grey (right).

This surprising phenomenon is not only interesting by its own, but also for its deeper meaning when related to real systems, for it may conceptually correspond to the so-called dichotomy “nature versus nurture”, that is, the updating dynamics can be thought of as the environment, whilst the local rule would represent the intrinsic properties of a system evolving from a particular initial condition. The behaviour of a system could strongly depend on the initial condition, or not at all. On the other hand, the same system may behave differently when interacting with different environments, that is, a system can be strongly dependent on the environment or, on the contrary, it can be robust to environment changes if its evolution is unaffected by them. Thus, this parallelism may lead to the discovery of environment-dependent versus environment-independent universal properties, and a deeper study of coalescence may help us to understand other phenomena, such as synchronisation and confluence.

As we can see, many properties of CA still need to be explored, studied, and understood, even for the most elementary cases. Moreover, some state-of-the-art characterisations are purely qualitative, so a rigorous mathematical analytical study should be done.

2 Definitions and notation

2.1 CA and ECA

Let us start with a general formalisation of the model that we are going to study:

Definition 2.1. A *cellular automaton* (CA) is given by a tuple (d, n, Q, V, f, α) where

- $d \in \mathbb{N}$ is the *dimension*;
- $n = (n_1, \dots, n_d) \in \mathbb{N}^d$ is the (possibly infinite) *size*;
- Q is the set of possible *states* that a cell may assume (the *alphabet*);
- $V = \{v_1, \dots, v_{|V|}\}$, the *neighbourhood*, is a finite set of vectors in \mathbb{Z}^d specifying which cells affect one another, that is, which cells takes into account the local transition rule f when updating the value of a cell. For $d = 1$ it is usually specified by its symmetric radius r , and then $V = \{-r, -(r-1), \dots, -1, 0, 1, \dots, r-1, r\}$;
- $f : Q^{|V|} \rightarrow Q$ is the *local transition function* or *rule*. It defines how the state of a cell is updated according to the states of the cells located in its neighbourhood;
- $\alpha \in [0, 1]$ is the *synchrony rate* which will determine the *global transition function* (see Section 2.2). That is, each cell has probability α to be updated (note that $\alpha = 0$ is an abuse of notation which corresponds to the extreme case where a single cell is updated at each time step).

However, we will most of the time focus on the simplest class of CA, namely elementary cellular automata:

Definition 2.2. An *elementary cellular automaton* (ECA) is a one-dimensional CA having two possible values for each cell and radius one (i.e. rules depend only on the cell being updated and its two nearest neighbours). Thus, it corresponds to the tuple $(1, n, \{0, 1\}, \{-1, 0, 1\}, f, \alpha)$ with $n \in \mathbb{N}$, $f : \{0, 1\}^3 \rightarrow \{0, 1\}$ and $\alpha \in [0, 1]$.

There are $2^{2^3} = 256$ such automata, each of which can be indexed according to its local transition rule. We use the classical notation (see Table 1) introduced by Wolfram [50] together with the alternative encoding (see Table 2) introduced by Fatès [17] which provides an immediate inference of the local behaviour of the CA just by looking at its letter code¹.

- In Wolfram's notation, a rule f is denoted by the number $2^7 f(1, 1, 1) + 2^6 f(1, 1, 0) + 2^5 f(1, 0, 1) + 2^4 f(1, 0, 0) + 2^3 f(0, 1, 1) + 2^2 f(0, 1, 0) + 2^1 f(0, 0, 1) + 2^0 f(0, 0, 0)$.

	2^7	2^6	2^5	2^4	2^3	2^2	2^1	2^0
$x y z$	111	110	101	100	011	010	001	000
$f(x, y, z)$	1	1	0	1	0	0	1	0

Table 1: This example of transition function corresponds to rule $210 = 11010010_2$.

¹Another original notation was proposed by Macauley et al. in [27] and used in their further works [26, 28].

- In Fatès' notation, a rule f is denoted by its difference to the identity automaton, using a concatenation of letters which specify the active transitions (the ones that change the state of the cell being updated; i.e. if $f(x, 0, y) = 1$ or $f(x, 1, y) = 0$) according to the following letter code: A corresponds to the neighbourhood 000, B to 001, C to 100, D to 101, E to 010, F to 011, G to 110, and H to 111.

	A	B	C	D	E	F	G	H
$x y z$	000	001	100	101	010	011	110	111
$f(x, y, z)$	0	1	1	0	0	0	1	1

Table 2: This example of transition function corresponds to rule BCEF, which is rule 210 in Wolfram's notation.

In the context of asynchronism, the advantage of this second naming is that we can deduce from it whether the local behaviour can increase the number of ones (transitions A, B, C, D) or decrease it (transitions E, F, G, H), whether it is possible that isolated zeros (resp. ones) disappear (transition D, resp. E) or appear (transition H, resp. A) and the displacement of 01 and 10 frontiers (transition B moves 01 to the left whilst transition F moves it to the right, and transition C moves 10 to the right whilst transition G moves it to the left) (see Table 3).

1	000	11010111	10	001	1010111	100	011010111	10001	101	0111	
	↓ A			↓ B			↓ C			↓ D	
	101011010111		1001111010111		110011010111		100011110111				
<hr style="width: 50%; margin: 10px auto;"/>											
	100011	010	111	100	011	010111	1000	110	10111	100011010	111
		↓ E			↓ F			↓ G			↓ H
	100011000111		100001010111		100010010111		100011010111				100011010111

Table 3: Examples of resulting configuration after the application of an active transition.

Note that this is the local behaviour of each possible transition if updated separately. The combination of several updates applied at the same time on the same neighbourhood can produce different global behaviours (see Note on page 10).

At each (discrete) time step, the CA configuration evolves according to its transition function (based on the states of neighbouring cells) and the updating scheme (see Section 2.2). The *space-time diagram* is the usual way to visualise the dynamics of a CA. For the one-dimensional case, it is obtained by stacking these successive configurations (see Figure 5).

Most analytical studies aim to find theoretical results for infinite-size CA. However, it is not always possible to experimentally handle that kind of CA. In order to get an insight into infinite-size CA, we can use *periodic boundary conditions*, so that for a dimension which has size n , each cell

can be indexed by $\mathbb{Z}/n\mathbb{Z}$. In that case, taking the same size n in every dimension we can denote the *cell space* by $U = (\mathbb{Z}/n\mathbb{Z})^d$. Then the *configuration space* may be defined as Q^U . That is, each *configuration* $x \in Q^U$ is a *word* indexed by U with *letters* in Q . A *zone* is a subset of consecutive cells being in the same state.

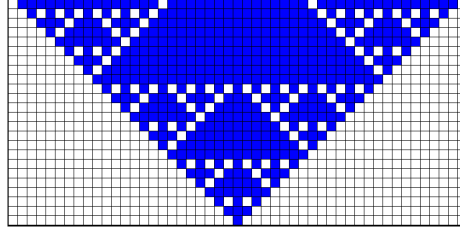


Figure 5: Space-time diagram of ECA 182 (BCDFG) starting from a configuration with a single one (blue cell) and where each cell is simultaneously updated at each time step. Time, thus, goes upwards.

When working with ECA, we denote by $|x|_1$ the number of ones in configuration x , and $|x|_{01}$ the number of alternations from zero to one in configuration x . Note that, using periodic boundary conditions, this is a counter of the number of zones and $|x|_{01} = |x|_{10}$. This notion can be generalised for any kind of CA and even for non-contiguous patterns as follows: let $y \in Q^W$, where $W \subseteq U$, be a pattern; we denote by $|x|_y = |\{i \in U : \forall j \in W, x_{i+j} = y_j\}|$ the number of occurrences of pattern y in configuration x .

Example 2.1. The configuration $x = 000011010111011001$ with periodic boundary conditions has 5 zero-zones, 5 one-zones, $|x|_{01} = |x|_{10} = 5$, $|x|_{1011} = 2$, and $|x|_{0*0} = 4$ with $* \in \{0, 1\}$.

These are the basic tools to study the behaviour of CA. However, recall that, informally speaking, we say that a CA is *coalescent* if, starting from two different initial configurations and updating the same cells at each time step, we obtain exactly the same configuration after letting it evolve for some time. As we could see on page 5 Figure 4 (left and centre), it is often difficult to visually detect coalescence just by comparing two space-time diagrams side by side, even when n is small. Thus, in order to study coalescence, we are going to use all the tools and notations introduced above together with what we call the *agreement space-time diagram*, which is the superimposition of two space-time diagrams showing the differences between both configurations (see page 5 Figure 4, right).

Remark. The agreement space-time diagram of two ECA is the space-time diagram of a 4-state one-dimensional CA: let $i \in \mathbb{Z}/n\mathbb{Z}$ and $x, y \in \{0, 1\}^{\mathbb{Z}/n\mathbb{Z}}$ be two configurations. Then a cell in its superimposition z can be in the following states:

$$z_i = \begin{cases} a_0 & \text{iff } x_i = y_i = 0 \\ a_1 & \text{iff } x_i = y_i = 1 \\ d_0 & \text{iff } x_i = 0 \text{ and } y_i = 1 \\ d_1 & \text{iff } x_i = 1 \text{ and } y_i = 0 \end{cases}$$

that is,

$$z \in \left\{ a_0 = \begin{pmatrix} 0 \\ 0 \end{pmatrix}, a_1 = \begin{pmatrix} 1 \\ 1 \end{pmatrix}, d_0 = \begin{pmatrix} 0 \\ 1 \end{pmatrix}, d_1 = \begin{pmatrix} 1 \\ 0 \end{pmatrix} \right\}^{\mathbb{Z}/n\mathbb{Z}}$$

and its local transition function f is fully determined by the local transition function of the ECA f_{ECA} :

$$f \left(\begin{pmatrix} x' \\ x \end{pmatrix}, \begin{pmatrix} y' \\ y \end{pmatrix}, \begin{pmatrix} z' \\ z \end{pmatrix} \right) = \begin{pmatrix} f_{ECA}(x', y', z') \\ f_{ECA}(x, y, z) \end{pmatrix}$$

where $x, x', y, y', z, z' \in \{0, 1\}$. Its global transition function, ring size and neighbourhood are the same as the original ECA. Thus, we see that studying ECA coalescence corresponds to the study of the 4-state CA defined above.

If the agreement space-time diagram corresponds to the space-time diagram of a binary (2-state) CA, we call it the *quotient rule* (see Figures 10 and 11 on pages 15 and 16), that is, we can study the agreement space-time diagram as if it were a 2-state CA the cells of which may be either in agreement or disagreement state.

2.2 Updating schemes and fixed points

There are different types of *updating schemes*, that is, different ways to choose which cells will be updated at each time step. These updating styles may radically change the global behaviour of the dynamics of a CA (see Figure 6) and, thus, its properties, like coalescence. The main updating schemes are:

- *Synchronous dynamics*: all cells are updated in parallel; that is, the transition function is simultaneously applied on each cell at each time step with probability $\alpha = 1$.

Historically, this is the most used and studied updating scheme because it was the one associated to the seminal definition of CA. However, there has been much interest in asynchronous regimes over the last decade [14].

- *Partially asynchronous dynamics*: each cell is independently updated with probability $\alpha \in (0, 1)$ at each time step. It is also known as *α -asynchronous dynamics*.

Partially asynchronous CA are a subclass of *probabilistic CA*, which have stochastic updating local rules [5, 6, 29].

- *Fully asynchronous dynamics*: at each time step, only one cell is randomly and uniformly chosen to be updated. Notice that this updating scheme can only be applied to finite-size CA; otherwise, we would need to consider continuous time. With a small abuse of notation we refer to it as $\alpha = 0$.

Fully asynchronous CA are a subclass of *interacting particles systems* (IPS), which are continuous-time Markov processes [5, 18, 24].

Note. Even though this last dynamics intuitively corresponds to the limit $\alpha \rightarrow 0$, note that it may not always coincide. For example, ECA 146 (BCEFG) starting from a configuration

...1111111100111111... and under fully asynchronism could never reach a configuration with all ones; however, under a partially asynchronous update with very small α , there is always a tiny possibility that the size two zero-zone disappears if the two consecutive cells having state 0 are updated simultaneously.

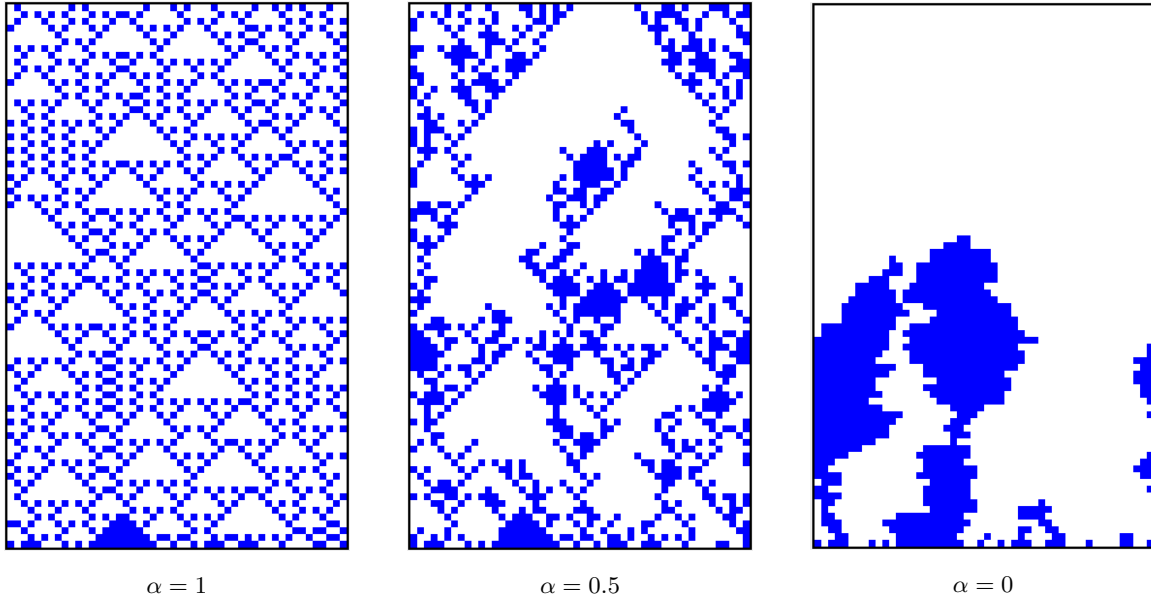


Figure 6: Space-time diagrams of ECA 146 (BCEFG) with periodic boundary conditions and $\alpha = 1$ (left), $\alpha = 0.5$ (centre), and $\alpha = 0$ (right), all starting from the same initial configuration. Note that, for the fully-asynchronous case (right), the k -th line from bottom to top corresponds to the configuration at time $t = nk$, where n is the size, whilst for the other dynamics, $t = k$ (centre and left).

Each updating scheme gives rise to a *global transition function*, $F_\alpha : Q^U \rightarrow Q^U$, which associates to each configuration $x \in Q^U$ a configuration $y \in Q^U$ according to the following definitions:

- For a synchronous updating scheme ($\alpha = 1$), $y_i = f(x_{i-1}, x_i, x_{i+1})$ for all $i \in U$.
- For a partially asynchronous updating scheme ($\alpha \in (0, 1)$), for every $i \in U$, $y_i = f(x_{i-1}, x_i, x_{i+1})$ with probability α and $y_i = x_i$ with probability $(1 - \alpha)$.
- For a fully asynchronous updating scheme ($\alpha = 0$), $y_i = f(x_{i-1}, x_i, x_{i+1})$ for a randomly uniformly chosen $i \in U$ and for each $j \neq i$, $y_j = x_j$.

We denote by x^t the configuration obtained after t applications of the given updating scheme; i.e., $x^t = F_\alpha^t(x)$. Note that for asynchronous updating schemes ($\alpha \in [0, 1)$) x^t is a random variable. It is important to notice that a reachable configuration under a given updating scheme may not be reachable under another one.

Remark. The complete set of configurations of a deterministic CA produced after any finite number of time steps can be described in terms of *regular formal language* [48].

Along its evolution, a CA may have more probability to reach some configurations than others, and there are some configurations from where any further application of the global transition function will result in the same configuration; i.e., it will remain constant. It will be important to identify these global behaviours in order to study and understand coalescence. In particular:

Definition 2.3. The set of *fixed points* of ECA f with a given n and synchrony rate α is $\{x \in Q^U : \mathbb{P}(F_\alpha(x) = x) = 1\}$.

Remark. The set of fixed points of the asynchronous dynamics is clearly identical to the set of fixed points of the synchronous dynamics. However, its reachability may vary depending on the updating scheme used.

Example 2.2. The set of fixed points of ECA 130 (BEFG) with ring size n is $\{0^n, 1^n\}$. Under synchronous updating, none of them is reachable from a configuration different from the fixed point itself. However, under fully asynchronous dynamics, ECA 130 converges very quickly to 0^n for any configuration different from 1^n .

We can easily determine the set of fixed points of an ECA by using an adaptation of *de Bruijn diagrams* (see Figure 7 and see e.g. [15]). It represents all the possible transitions in a graph form, allowing us to easily detect all possible cycles corresponding to fixed points configurations (we can find the set of fixed points of all ECA in Table 5 of Appendix A). Informally speaking, any cycle of inactive transition nodes will be a fixed point, because they correspond to static configurations.

Example 2.3. From a de Bruijn diagram we can deduce that the set of fixed points of ECA 45 (ADGH) with ring size $n = 3k$ is $\{(001)^k\}$ because the only possible cycle of inactive transitions (B, C, E, F) is BEC. Note that this fixed point will be impossible to reach if $n \neq 3k$, where $k \in \mathbb{N}$. Using the same procedure we can see that the set of fixed points of ECA 44 (DGH) with ring size n is $\{0^n, 10^{r_1}10^{r_2} \dots 10^{r_q} \text{ with } r_i \geq 2 \text{ and } \sum_{i=1}^q r_i = n - q\}$, because the only possible cycles of inactive transitions (A, B, C, E, F) are the A loop and $A^m\text{BEC}$, where $m \in \mathbb{N}$ can be different each time we come back to node C. Note that 0^n cannot be reached from any configuration different from 0^n for both synchronous and fully asynchronous updating schemes.

Definition 2.4. The *worst expected convergence time* of a fully asynchronous ECA f ($WECT_f$) can be defined as follows: let $x \in Q^U$, let \mathcal{S}_f be the set of fixed points of rule f , and let $\mathcal{T}_f(x) = \min\{t : x^t \in \mathcal{S}_f\}$ be the random variable representing the time needed to reach a fixed point starting from configuration x under fully asynchronous dynamics. Then $WECT_f = \max_{x \in Q^U} \mathbb{E}[\mathcal{T}_f(x)]$ (see [17]).

2.3 ECA properties

2.3.1 Symmetries and equivalence classes

It is easy to see that there is a total of 88 fundamentally non-equivalent ECA rules after basic symmetry considerations (see Table 5 in Appendix A). These symmetries that have been classically considered are the following simple transformations: vertical reflection, conjugation (interchange

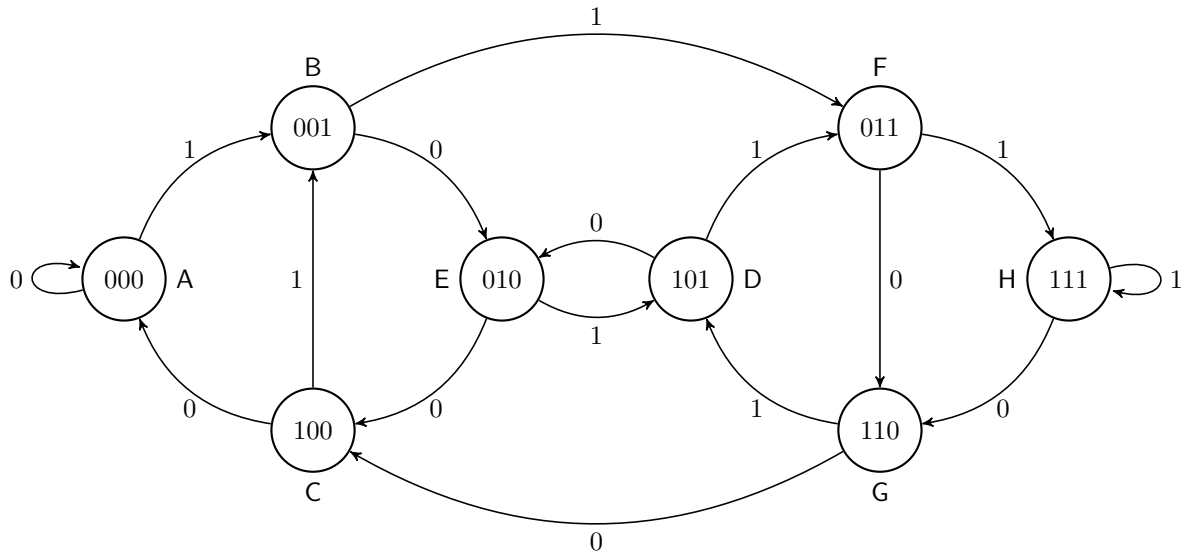


Figure 7: De Bruijn diagram representing all possible transitions of an ECA. Each node is one of the eight possible neighbourhoods (labelled with the letter code presented in Table 2 on page 7). Each path of length k corresponds to a possible configuration of size $n = 3 + k$. Each cycle corresponds to a possible fixed point.

of 0 and 1), and the combination of these two operations (see Figures 8 and 9). Since their main properties (including coalescence) are unaffected by these transformations, ECA form 88 equivalence classes, each of which is represented by the *minimal* ECA of the class; i.e., the lowest-numbered using Wolfram’s notation (see Table 1 on page 6).

This is important to know and very useful, because it notably reduces the study cases, for we can deal with these 88 representative ECA without loss of generality. That is, we know that any result that applies to an ECA can be extended to the other ECA in its equivalence class.

Using Fatès’ notation we can observe that the classical symmetries considered correspond to the following changes in the letter code:

- *Vertical reflection* corresponds to the exchanges $B \leftrightarrow C$ and $F \leftrightarrow G$.
- *Conjugation* corresponds to the exchanges $A \leftrightarrow H$, $B \leftrightarrow G$, $C \leftrightarrow F$ and $D \leftrightarrow E$.
- The *composition* of both transformations corresponds to the exchanges $A \leftrightarrow H$, $B \leftrightarrow F$, $C \leftrightarrow G$ and $D \leftrightarrow E$.

As we can see in Figure 8, ECA 2 (BEFGH) is equivalent to ECA 16 (CEFGH) under vertical reflection, ECA 191 (ABCDG) under conjugation, and ECA 247 (ABCDF) under the composition of both transformations. Another example with a less trivial behaviour is given in Figure 9.

2.3.2 Linearity, affinity, quiescence, homogeneity and universality

There are several special classes of ECA with interesting and useful properties.

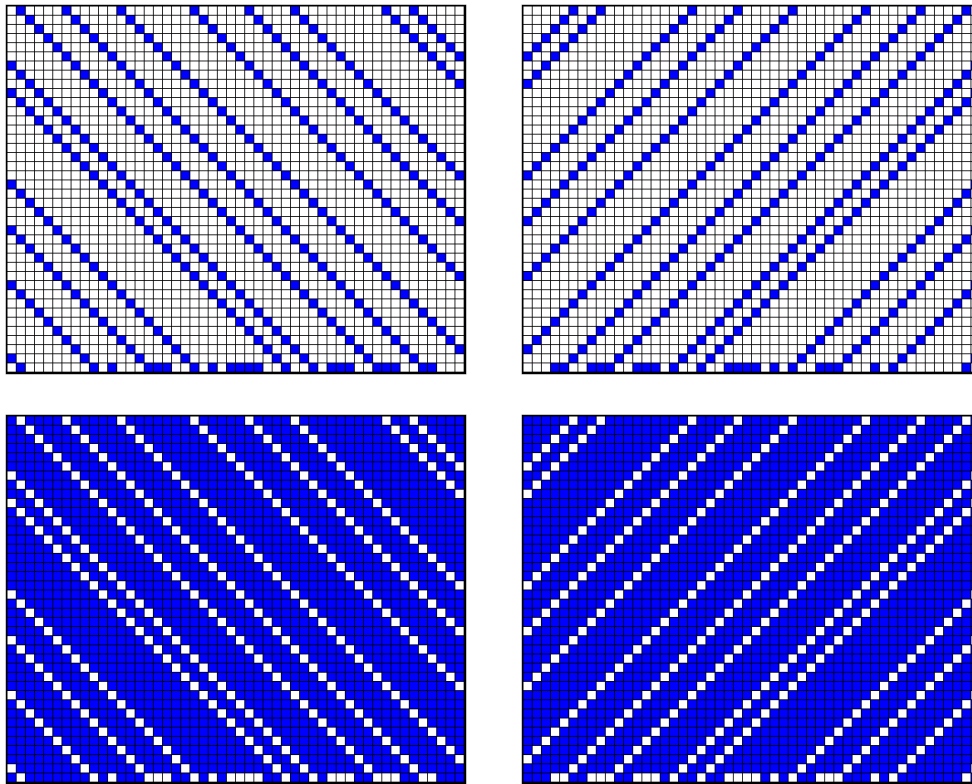


Figure 8: Space-time diagrams of four equivalent ECA with periodic boundary conditions. Changing the initial configuration accordingly and using synchronous updating, we can see that ECA 2 (top left) is indeed equivalent to ECA 16 (top right) under reflection, to ECA 191 (bottom left) under conjugation, and to ECA 247 under both reflection and conjugation.

Definition 2.5. *Linear* ECA are those that can be described by a linear rule; that is, their rules can be expressed as $f(x_1, x_2, x_3) = \sum_{i \in I} x_i \pmod 2$ where $I \subseteq \{1, 2, 3\}$.

There are 8 such automata: 0, 60, 90, 102, 150, 170, 204, 240.

Remark. Local transition functions of linear ECA behave as XOR (exclusive disjunction); i.e., they perform sum modulo 2.

Definition 2.6. *Additive* or *affine* ECA are those that can be described by an affine rule; that is, its rule can be expressed as $f(x_1, x_2, x_3) = \epsilon + \sum_{i \in I} x_i \pmod 2$, where $I \subseteq \{1, 2, 3\}$ and $\epsilon \in \{0, 1\}$.

There are 16 such automata: 0, 15, 51, 60, 85, 90, 102, 105, 150, 153, 165, 170, 195, 204, 240, 255.

Remark. Additive ECA correspond to XOR and NXOR operations over the neighbourhood.

Notice that the set of linear ECA is a subset of the set of additive ECA.

Lemma 2.1 ([42, page 6]). *For both asynchronous dynamics, affine ECA rules are exactly the rules for which the agreement space-time diagram is the space-time diagram of an elementary cellular automaton.*

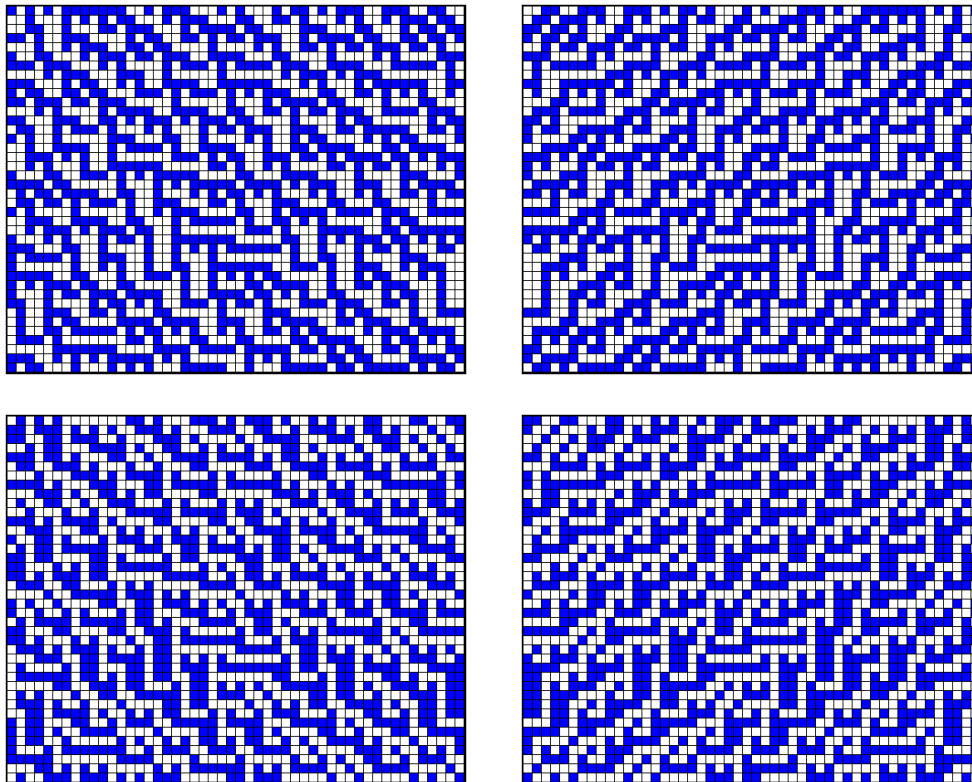


Figure 9: Space-time diagrams of four equivalent ECA with periodic boundary conditions. Changing the initial configuration accordingly and using synchronous updating, we can see that ECA 45 (top left) is indeed equivalent to ECA 101 (top right) under reflection, to ECA 75 (bottom left) under conjugation, and to ECA 89 under both reflection and conjugation.

Thus, the quotient rule of an additive ECA is the linear ECA obtained from the same rule with $\epsilon = 0$ (see Figure 10), and for both asynchronous dynamics, the agreement space-time diagram of linear rules is the space-time diagram of the rule itself, in other words, the quotient rule of a linear ECA is itself (see Figure 11).

Remark. This notion of additivity can be generalised as follows: let F_α be an ECA, $x, y \in Q^U$ two configurations, and \oplus a binary operator on Q . Then F_α is an additive ECA with respect to \oplus if $F_\alpha(x \oplus y) = F_\alpha(x) \oplus F_\alpha(y)$ for any x and y [50].

Definition 2.7. A state $q \in Q$ is *quiescent* if $f(q, q, q) = q$. An ECA is *doubly quiescent* (DQECA) if both states 0 and 1 are quiescent.

Remark. The number of regions in a fully asynchronous DQECA configuration cannot increase.

Remark. Any DQECA of size n has at least two fixed points: 0^n and 1^n .

Definition 2.8. An ECA F_α is *nilpotent* if all configuration eventually reach the same quiescent state; that is, if for any ring size n and $\forall x \in Q^U$, $\exists q \in Q$ and $\exists T \in \mathbb{N}$ such that $\forall t \geq T, F_\alpha^t(x) = q^U$ (for more details, see [21, 29]).

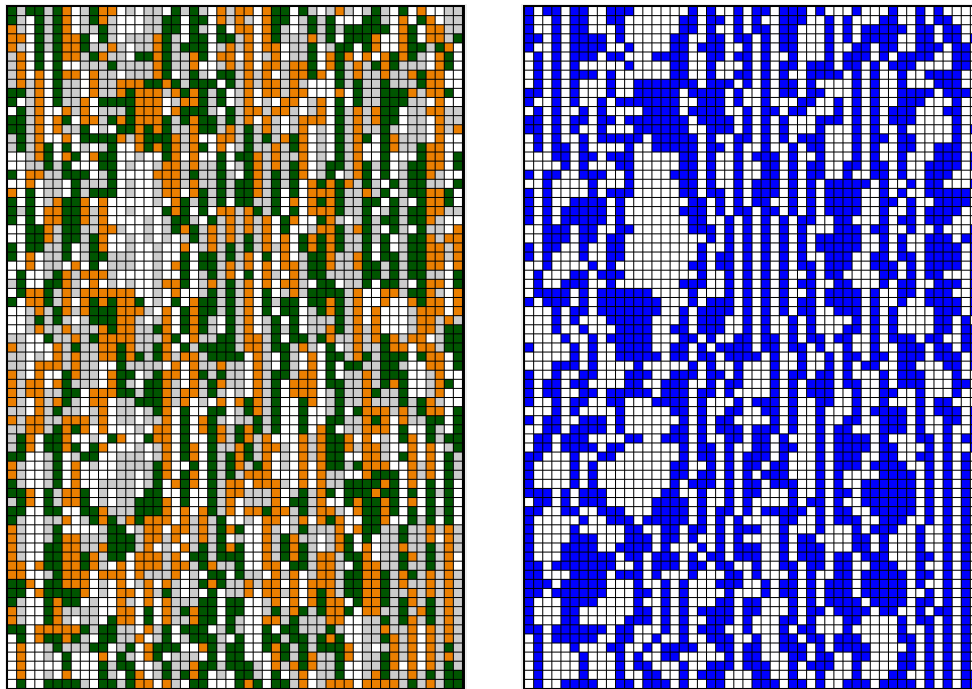


Figure 10: We can see that the agreement space-time diagram of fully asynchronous ECA 105 (left), exactly corresponds to the space-time diagram of ECA 150 (right). Thus, ECA 150 is the quotient rule of ECA 105.

However, the notion of nilpotency does not capture the behaviour of CA that can reach multiple quiescent states, here DQECA. This is an interesting behaviour where all initial information is removed, like in the nilpotent case, because any configuration will lead to one of the two possible homogenous states, and it will be of great importance when studying coalescence, so we defined it as follows:

Definition 2.9. An ECA F_α is *homogenising* if for any ring size n and $\forall x \in Q^U$,

$$\mathbb{P}(\exists q \in Q, \exists T \in \mathbb{N} : \forall t \geq T, F_\alpha^t(x) = q^U) = 1.$$

Remark. An ECA may be homogenising under a particular updating style, but this does not imply that it will be homogenising under another kind of updating scheme (see Figure 12).

Definition 2.10. An ECA is *universal* if it is capable of arbitrarily complex behaviour and so able to perform computations of arbitrary sophistication. In particular, given appropriate initial conditions, it can be effectively programmed to emulate any possible CA.

Remark. ECA 110 (124, 137, 193) are proven to be universal. Wolfram suggested that 27 out of 256 may be universal [50].

Remark. It has been shown that asynchronous CA can simulate arbitrary synchronous CA (by extending the number of states, the dimension or the size of the neighbourhood, for example). From

this result a universal asynchronous CA can be easily constructed (see e.g. [23, 25, 32–34, 36, 37] for further insight and [14, 51] for discussions on the issue).

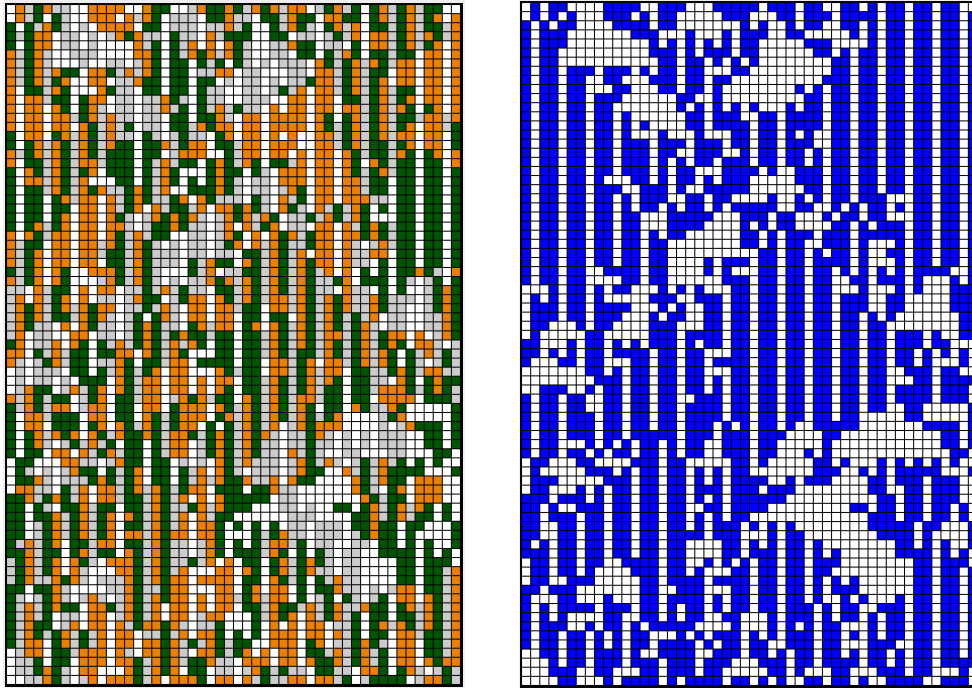


Figure 11: The agreement space-time diagram of fully asynchronous ECA 90 (left), is equal to the space-time diagram of the same rule (right). Thus, applying exactly the same sequence of updates, the quotient rule of ECA 90 is itself.

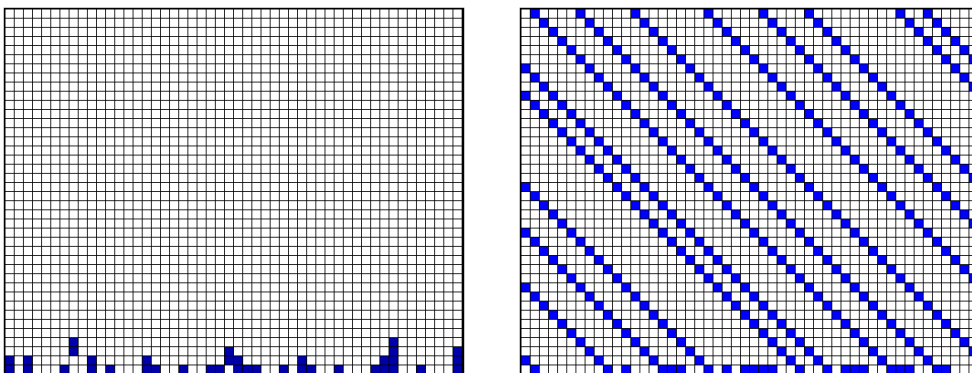


Figure 12: ECA 2 is homogenising under fully asynchronous dynamics (left) but not under a synchronous updating scheme (right).

3 Precedings

The starting point of this research project is Rouquier's PhD thesis [38] and, in particular, one of its chapters rewritten as an article that focuses on coalescing CA [42]. In this paper, Rouquier and Morvan coin the term *coalescence* and first define it as follows: *an asynchronous finite CA is coalescing if, for any two initial configurations, applying the same sequence of updates leads both configurations to become identical within polynomial expected time (with respect to n)*. Notice that for a CA to be coalescent it is required that it coalesces quickly enough. This definition aimed to formalise the first observations of this phenomenon that appeared in [16]. They formally study the behaviour of six asynchronous ECA and give proofs to the following results:

- The identity rule 204 cannot coalesce.
- For both asynchronous dynamics, 60 is not coalescing.
- 6 and 7 are coalescing for the fully asynchronous dynamics when n is odd.
- 15 and 170, for both asynchronous dynamics, either coalesce or end in total disagreement, each case with probability $\frac{1}{2}$.

They also show how to construct coalescing CA with arbitrarily many states. Next, their simulation study of all partially asynchronous ECA is presented and, using the asymptotic density, all rules are classified with respect to coalescence in the following categories:

- a) CA that never coalesce.
- b) CA that coalesce rapidly in a trivial way (they converge to a unique fixed point).
- c) CA that coalesce rapidly to non trivial orbits.
- d) CA that combine a), b) and c) depending on α .
- e) CA that end in either full agreement between configurations (coalescence) or full disagreement, depending on the sequence of updates and the initial configuration.
- f) CA that combine e) with either a) or c).

Finally, the authors study the transition between non coalescence and coalescence when α varies for the ECA that combine a) and c), and show that they present a phase transition (abrupt change in macroscopic properties of a system with only a small change of a control parameter around a critical value) belonging to the universality class of directed percolation (see also [13]).

Other articles fundamental to our work are [17], where Fatès et al. analytically study the convergence time of all DQECA which inspired our formal study, and [16], where Fatès and Morvan use a statistical approach with macroscopic parameters in order to experimentally study the robustness to asynchronism of ECA and which inspired our qualitative study.

In order to explore CA's dynamics, we used FiatLux², a Java based software developed by Fatès which allows one to simulate different kinds of 1D and 2D CA, using different updating dynamics and different topologies.

²The applet is available on <http://fiatlux.loria.fr>.

4 Visualisation and qualitative exploration

We considered that studying ECA instead of trying to find general results for any kind of CA was a good starting point. Moreover, we focused on fully asynchronous dynamics because phase transitions have been observed in partially asynchronous ECA [13, 16, 42], and so their complete analytical study would go beyond the scope of this project.

Before analytically study coalescence, we qualitatively explored the behaviour of all fully asynchronous ECA and their coalescence. This work allowed us to detect quick coalescence (in linear or even logarithmic time), coalescence to a fixed point, coalescence before reaching a fixed point, coalescence to a non trivial configuration, slow coalescence, and different kinds of non-coalescent behaviour (see Figure 13).

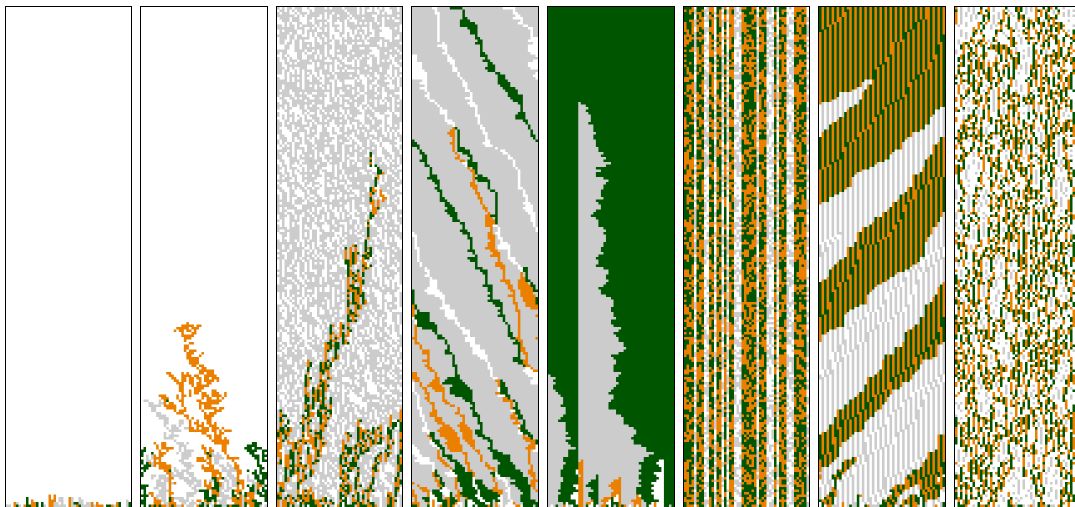


Figure 13: Qualitatively different examples of different coalescence styles. From left to right, ECA 40, 58, 62, 154, 184, 51, 14 and 1.

The first exploration work was done by comparing two space-time diagrams of the same ECA under the same fully asynchronous dynamics (fixing a seed for the random sequence of updates, we can force both ECA to update the same cells at each time step) and starting from two different random configurations. We explored the behaviour of the system with different ring sizes and different initial conditions (random or particular ones). We repeated these experiments several times in order to evaluate their dependence on the updating sequence.

After that, we developed a new feature of FiatLux allowing us to display the agreement space-time diagram of two ECA, and we repeated the exploration by using this new tool. This visualisation provides further insight into the coalescence style because it displays the dynamics of the disagreement, which may not be straightforward from the side-by-side comparison of two or several space-time diagrams.

By using it, we could quickly verify our previous results and intuitions and, together with an exhaustive study of ECA fixed points, we were able to distinguish trivial from non-trivial coalescence. Furthermore, we could already find some particular configurations and sizes that altered the predominating coalescence behaviour (see Figure 14 and Figure 15). Finally, incrementing the size of the CA, we could also detect coalescent behaviour produced by the use of periodic boundary conditions (see Figure 16).

Thus, this qualitative study allowed us to roughly classify all ECA according to their predominating coalescence behaviour (see Table 5 of Appendix A).

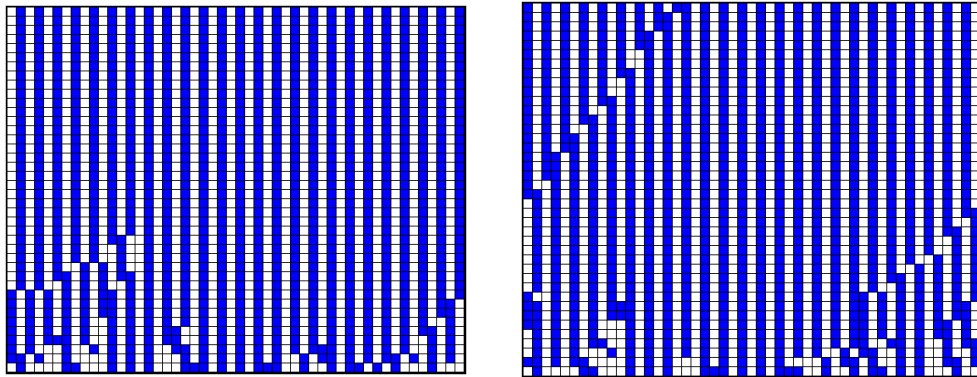


Figure 14: ECA 15 with periodic boundary conditions and under fully asynchronous dynamics with an even ring size of $n = 50$ is able to reach the fixed point $(01)^{n/2}$ (left) but this configuration is unreachable when an odd ring size of $n = 49$ is used (right).

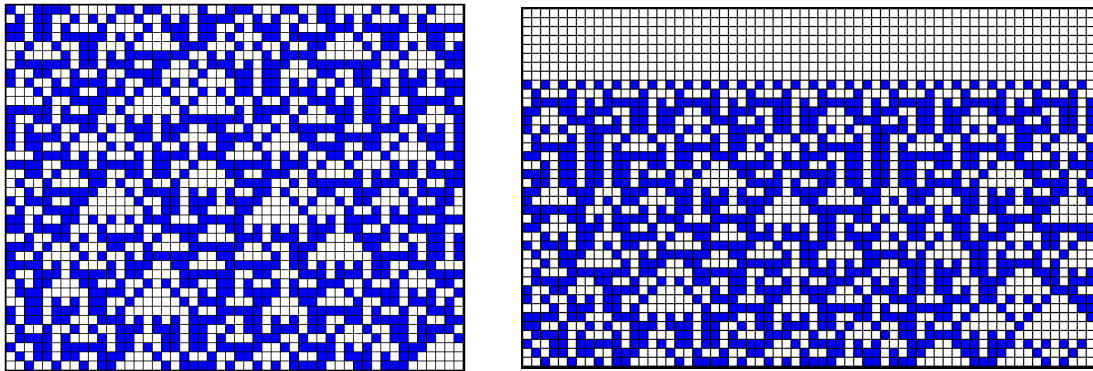


Figure 15: ECA 90 with periodic boundary conditions and under synchronous dynamics with ring size $n = 50$ (left) and ring size a power of two, like $n = 64$ (right), have a completely different asymptotic behaviour.

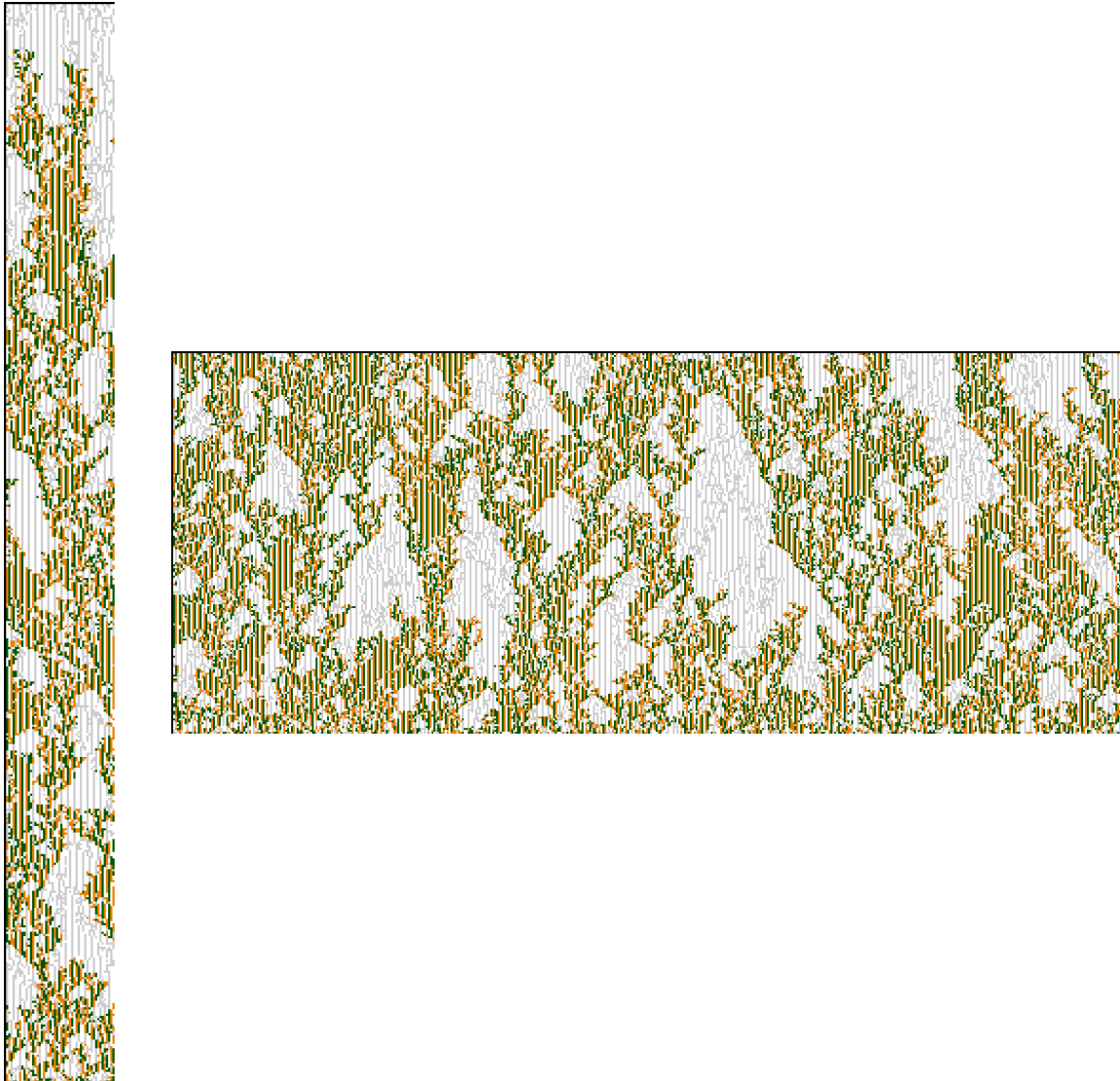


Figure 16: ECA 37 with periodic boundary conditions and under fully asynchronous dynamics with ring size $n = 50$ (left) and ring size $n = 500$ (right), where we can note that the coalescence of the first is apparent and due to the effect of periodic boundary conditions.

5 Definitions of coalescence behaviours

In order to analytically study coalescence, first of all we need to define this concept formally.

Let $(x^t, y^t) = F_0^t(x, y)$ denote the random evolution of two configurations updating the same cell at each time step and starting from the initial configurations $x = x^0, y = y^0 \in S \subseteq Q^U$. Then we denote by $T_{xy} = \inf\{t \geq 0 : x^t = y^t\}$ the random variable representing the first time that the two configurations coincide, that is, the minimum number of time steps needed to observe coalescence.

Definition 5.1. We say that a CA *coalesces* in time $t(n)$ if, for *any* two initial configurations, applying the same sequence of updates leads both configurations to become identical within expected time $t(n)$. Formally, if $\forall x, y \in Q^U$, $\mathbb{E}[T_{xy}] \leq t(n)$.

Notice that this definition includes the extreme case of a CA that only coalesces in “infinite” time, due to its stochastic nature. Informally speaking, these systems have the potential to coalesce but this outcome is highly unlikely. However, if given enough (infinite) time, they will eventually coalesce “by chance”. This definition excludes CA that will never coalesce, not even after an infinite time; for example, the identity rule ECA 204. Figure 17 gives several examples of coalescence reached in different times that inspired this definition.

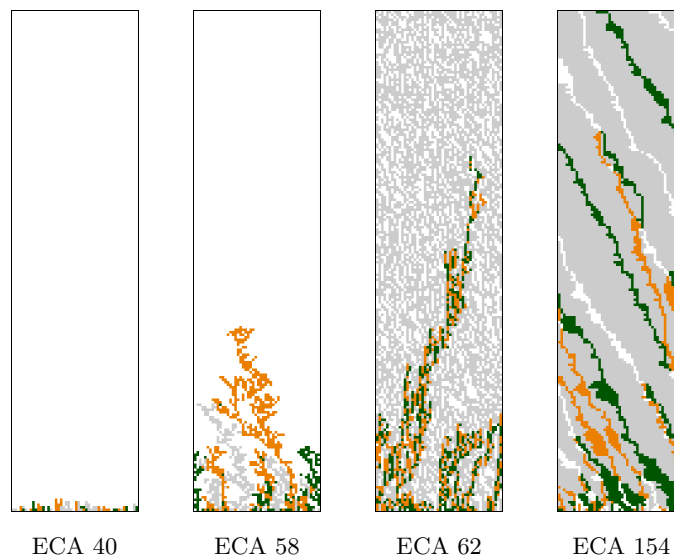


Figure 17: All depicted ECA have periodic boundary conditions and fully asynchronous dynamics. From left to right, coalescence reached in logarithmic ($\mathcal{O}(\log n)$), logarithmic ($\mathcal{O}(\log n)$), linear ($\mathcal{O}(n)$) and quadratic times ($\mathcal{O}(n^2)$).

Remember that, in our presentation, what we consider 1 time step of the fully asynchronous dynamics actually corresponds to n time steps. If we chose to consider a single updated per represented time step, then the convergence time that we obtain should be multiplied by n .

Definition 5.2. We say that a CA is *trivially coalescent* in time $t(n)$ if its asymptotic behaviour is independent of *both* the initial configuration and the sequences of updates. That is, if starting from any two initial configurations and applying different updating sequences still leads both configurations to become identical within expected time $t(n)$.

Figure 18 shows several examples of trivial coalescence.

When we talk about *asymptotic behaviour*, we informally mean after the system evolved “long enough”, meaning that its behaviour will not be substantially different from the one already observed. The simplest examples to illustrate this concept are when a CA becomes independent of its initial condition (which can be seen as a perturbation or forced state) or reaches a fixed point (where it will

remain forever in a static configuration). The asymptotic behaviour of a CA may appear intuitive from an experimental point of view, but it may easily lead to false or inaccurate statements. It is quite difficult to analytically work with this notion, but a starting point is to use macroscopic parameters (such as the density of one state averaged over 10^6 time steps) and take a statistical approach.

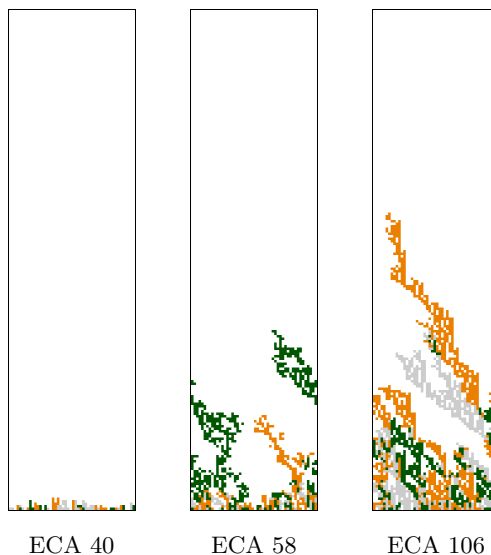


Figure 18: Examples of trivial coalescence. All depicted ECA have periodic boundary conditions and fully asynchronous dynamics.

There are several CA that are coalescent in general but they do not coalesce for some specific configurations. For example, taking an unreachable fixed point as one of the initial configurations leads to non-coalescence. Thus we define the following behaviour:

Definition 5.3. We say that a CA coalesces for a proper subset $S \subsetneq Q^U$ of initial configurations in time $t(n)$ if it is coalescent in time $t(n)$ when restricted to this subset of initial configurations, and it is not coalescent for the complementary set $\bar{S} = Q^U \setminus S$.

Figure 19 shows an example of an ECA coalescent for $S = Q \setminus \{1^n\} = \bar{1}^n$; i.e. an ECA having two fixed points: one (1^n) unreachable from any configuration different from the fixed point itself, and the other one (0^n) reachable from any other configuration.

We saw that the ring size may drastically affect the behaviour of a CA (recall Figure 14 and Figure 15) and, thus, its properties such as coalescence, so we can similarly define the following notion:

Definition 5.4. We say that a CA coalesces for a subset $N \subsetneq \mathbb{N}$ of ring sizes in time $t(n)$ if it is coalescent in time $t(n)$ when restricted to this subset of ring sizes, and it is not coalescent for the complementary set $\bar{N} = \mathbb{N} \setminus N$.

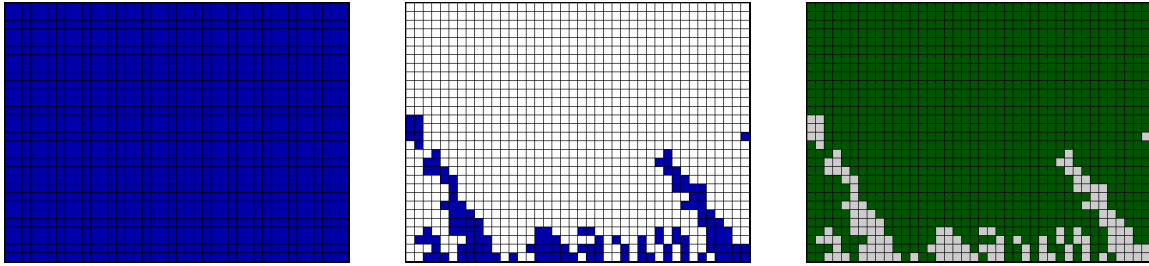


Figure 19: Space-time diagrams of ECA 130 with periodic boundary conditions and under fully asynchronous dynamics with initial configuration the fixed point 1^n (left) and starting from a random initial configuration (centre). Agreement space-time diagram showing that full disagreement is quickly reached (right).

Some CA, for example those with more than one reachable fixed point, may sometimes coalesce but sometimes not or even reach full disagreement. In order to capture this behaviour we define the following concept:

Definition 5.5. We say that a CA is coalescent with probability p if coalescence is reached with probability p and non coalescence with probability $1 - p$.

Figure 20 shows an example of an ECA that has two reachable fixed points $\{0^n, 1^n\}$. Thus, if both copies end up in the same fixed point, we will observe coalescence. On the other hand, if they converge to different fixed points we will observe full disagreement. The (non) coalescence of ECA presenting this kind of behaviour will most probably depend on the initial configuration.

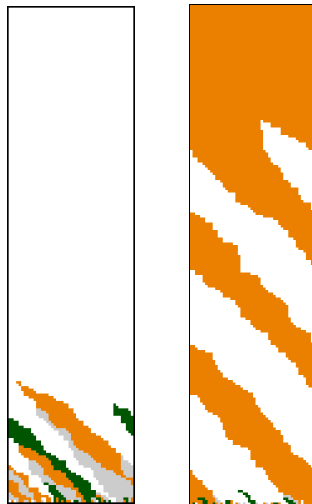


Figure 20: Agreement space-time diagrams of ECA 170 with periodic boundary conditions and under fully asynchronous dynamics reaching full agreement (left) and reaching full disagreement (right).

In particular, some ECA that coalesce with probability p may reach a non coalescent configuration where one of the copies is a translation of the other. Thus:

Definition 5.6. We say that a CA is *shift-coalescent* in time $t(n)$ if after letting it evolve $t(n)$ time steps, there exists a $j \in U$ such that $x_i^{t(n)} = \{y^{t(n)}\}_{i-j}$ for all $i \in U$.

Figure 21 shows an example of an ECA that may reach a non coalescent state where one configuration is a shift of the other.

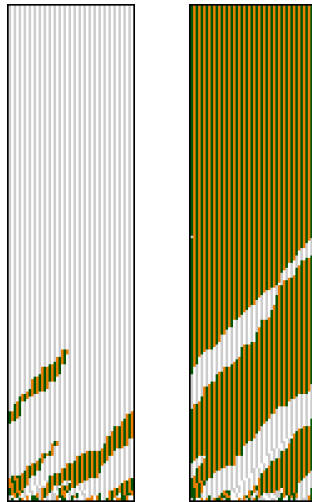


Figure 21: Agreement space-time diagrams of ECA 15 with periodic boundary conditions and under fully asynchronous dynamics reaching full agreement (left) and reaching full disagreement where one configuration is a shift of the other (right).

Notice that this probability p of reaching (shift) coalescence will, in general, be very difficult to determine because of CA's global behaviour complexity and because it should be averaged over every possible initial condition and every possible updating sequence.

Finally, the behaviour of some CA suggests that they might be able to coalesce if they were not forced to update exactly the same cells, because they tend or are very close to reach a coalescent state but this is sometimes impossible because of some differences that cannot be "broke" if both copies follow the same updating sequence (see Figure 22).

Thus, it would be interesting to study the notion of *coalescence percentage*, which could be an indicator to spot these cases and maybe some other properties related to coalescence. For example, the average coalescence percentage of a CA may be constant over time and for any initial condition, and this would be a clear indicator of non coalescence.

Definition 5.7. At each time step, the *coalescence percentage* is defined as the ratio $\frac{a}{n}$, where n is the ring size and a is the number of agreeing cells.

If needed, this measure could be averaged for all runs or measured after letting CA evolve for some time.

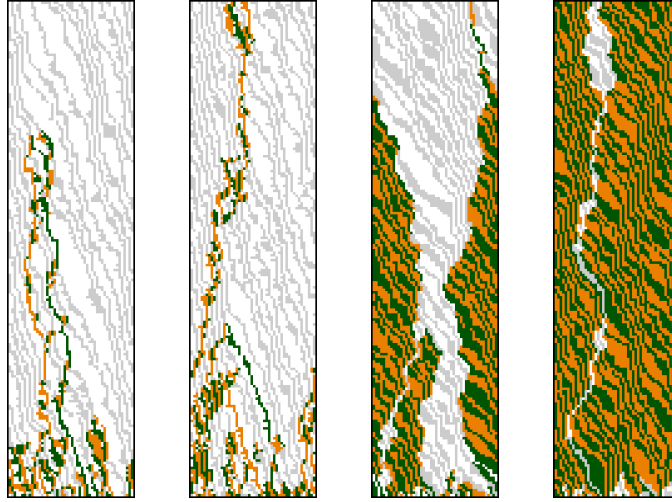


Figure 22: From left to right, agreement space-time diagrams with periodic boundary conditions and under fully asynchronous dynamics of ECA 134 reaching coalescence, ECA 134 unable to reach full coalescence because of some small remaining disagreement, ECA 142 very close to coalescence but unable to reach it, and ECA 142 very close to full disagreement.

6 Analytical tools

In order to formally prove some results we will need the following probabilistic notions and results.

Let $\epsilon > 0$, $m, m' \in \mathbb{N}$, and $(X_t)_{t \in \mathbb{N}}$ be a sequence of random variables taking values in $\{-m, \dots, m'\}$. Let $\Delta X_t = X_t - X_{t-1}$ and $(\mathcal{X}_t)_{t \in \mathbb{N}}$ be the sequence of past values taken by previous random variables up to t . The following lemma bounds the convergence time of a random variable that decreases on expectation.

Lemma 6.1 ([17]). *Assume that if $X_t > 0$, then $\mathbb{E}[\Delta X_{t+1} | \mathcal{X}_t] \leq \epsilon$. Let $T = \min\{t : X_t \leq 0\}$ denote the random variable corresponding to the first time t that $X_t \leq 0$. Then, if $X_0 = x_0$,*

$$\mathbb{E}[T] \leq \frac{m + x_0}{\epsilon}.$$

Let $(X_t)_{t \in \mathbb{N}}$ be now a sequence of random variables taking values in $\{0, \dots, m\}$.

Definition 6.1 ([17]). We say that $(X_t)_{t \in \mathbb{N}}$ is a *martingale of type I* if for all t :

- $\mathbb{E}[X_{t+1} | \mathcal{X}_t] = X_t$, and
- if $0 < X_t < m$, then $\mathbb{P}(\Delta X_{t+1} \geq 1 | \mathcal{X}_t) = \mathbb{P}(\Delta X_{t+1} \leq -1 | \mathcal{X}_t) \geq \epsilon$.

Let $T = \min\{t : X_t \in \{0, m\}\}$ denote the random variable corresponding to the *convergence time* of a type I sequence (X_t) to one of the two only possible fixed points. The following lemma bounds the convergence time of this random process.

Lemma 6.2 ([17]). *For any type I sequence (X_t) , if $X_0 = x_0$, the expectation of T satisfies*

$$\mathbb{E}[T] \leq \frac{x_0(m - x_0)}{2\epsilon}.$$

Finally, we will also need the following concepts:

Definition 6.2. Let f be a function with domain M and a partially ordered set (N, \leq) as codomain, and let g be a function defined on domain M and having the same codomain (N, \leq) . Then g is an *upper bound* (resp. *lower bound*) of f if $g(x) \geq f(x)$ (resp. $g(x) \leq f(x)$) for each $x \in M$. An upper or lower bound is said to be *sharp* if equality holds for at least one value of $x \in M$. An upper bound (resp. lower bound) is said to be *tight*, a *least upper bound* (resp. *greatest lower bound*) or a *supremum* (resp. *infimum*) if no smaller value or function is an upper bound (resp. lower bound).

We call *energy function* a real-valued function giving values to the sequence of random variables (X_t) according to its constraints, allowing us to construct a suitable (X_t) in order to apply the previously stated lemmas.

7 Analytical study

In this section we will only refer to the minimal representatives of the 88 ECA equivalence classes, but remember that any result proven for one ECA can be easily extended to the other members of its class.

7.1 Fixed points and homogenising ECA

Using a de Bruijn diagram (see page 12) we were able to determine all possible fixed points of all ECA (see Table 5 of Appendix A). The subset of minimal ECA having a non-empty set of fixed points $\mathcal{S} \subseteq \{0^n, 1^n\}$ is: $\{0, 2, 8, 10, 18, 24, 26, 32, 34, 38, 40, 42, 46, 50, 54, 56, 58, 60, 62, 106, 110, 122, 126, 128, 130, 136, 138, 146, 152, 154, 160, 162, 168, 170, 178, 184\}$. From this list we would like to determine the set of homogenising ECA under synchronous dynamics and under fully asynchronous dynamics.

First of all we perform a qualitative exploration in order to find any configuration that would provide a counterexample to the hypothesis that all ECA listed above are possible homogenising candidates.

For the synchronous case, it is easy to find counterexamples for ECA 2, 10, 24, 26, 34, 38, 42, 46, 50, 56, 58, 62, 110, 130, 138, 152, 154, 162, 170, and 178 because in general they present a cyclic evolution. We find counterexamples for ECA 32, 40, 160, and 168 if initialised with a $(01)^{n/2}$ pattern. ECA 18, 54, 60, 106, 122, 126, and 146 present a more complex behaviour, because they present some moving non-trivial structures or self-similarity. However, it is easy to obtain a cyclic evolution providing a counterexamples if initialised with a periodic pattern. In particular, some of the counterexamples we found are: ECA 18, 54, 146 initialised with $(0011)^{n/4}$ with $n = 4k, k \in \mathbb{N}$, ECA 60 initialised with $(010)^{n/3}$ with $n = 3k, k \in \mathbb{N}$, ECA 106 and 122 initialised with $(01)^{n/2}$, and ECA 126 initialised with $(0111)^{n/4}$ with $n = 4k, k \in \mathbb{N}$. ECA 0 and 8 are proven to be the only two nilpotent ECA (see e.g. [46]). Thus, they are homogenising. ECA 128 (EFG) is doubly quiescent and has fixed points $\{0^n, 1^n\}$ (see page 14). If we start from a configuration different from the fixed point 1^n there must be at least one 0. Looking at its letter code we clearly see that the size of any

present zero-zone can only increase, we also know that the number of zones cannot increase and that a one-zone can disappear once it has size 2 or 1. Thus, ECA 128 is homogenising. Finally, using a similar reasoning than for ECA 128, we can easily conclude that ECA 136 (EG) is also homogenising.

From this study we are able to deduce that the set of homogenising ECA under synchronous dynamics is $\{0, 8, 128, 136\}$ together with their symmetric ECA.

For the fully asynchronous case, we start by determining the reachability of the set of fixed points of each ECA. With this information we can already detect some non-homogenising ECA. In particular, it is impossible that ECA 38 (BDFGH), 46 (BDGH), 54 (BCDFGH), 60 (CDGH), 62 (BCDGH), 110 (BDH), and 126 (BCDH) are homogenising because their only fixed point is $\{0^n\}$ but under fully asynchronous updating it is unreachable from any configuration different from the fixed point itself, because an isolated 1 (last configuration before reaching the fixed point) could never disappear (E is not active). It is clear that ECA 0 (EFGH) and ECA 8 (EGH) are homogenising. Using the analytical study and results in [17] we can easily deduce that fully asynchronous ECA 128, 130, 136, 138, 146, 152, 154, 160, 162, 168, 170, 178, and 184 are homogenising. Finally, we *conjecture* that the remaining ECA (listed in Table 4) are homogenising because (a) their only fixed point, which is reachable, is $\{0^n\}$; (b) most of them have more active transitions that increase the number of zeros; and (c) all of them have both transitions E and H active. Thus, even if their coalescence to the fixed point could be in theory very slow, they will always eventually reach 0^n . This hypothesis is in accordance with what we observe when modelling these ECA because all except for ECA 122 converge very quickly to the fixed point. On the other hand, we think that ECA 122 could have exponential or even infinite convergence time. However, in order to formally prove this claim we would need to formally demonstrate that these rules will always converge to 0^n for *any* ring size n and *any* initial configuration.

10	BEGH	2	BEFGH	18	BCEFGH	50	BCDEFGH
24	CEGH	32	DEFGH	34	BDEFGH		
40	DEGH	26	BCEGH	58	BCDEGH		
106	BDEH	42	BDEGH				
		56	CDEGH				
		122	BCDEH				

Table 4: List of ECA conjectured to be homogenising. They are listed together with their letter code, arranged in columns according to the number of active transitions, and sorted out by the number of active transitions that increase the number of ones.

Thus, we conjecture that the set of homogenising ECA under fully asynchronous dynamics, is $\{0, 2, 8, 10, 18, 24, 26, 32, 34, 40, 42, 50, 56, 58, 106, 122, 128, 130, 136, 138, 146, 152, 154, 160, 162, 168, 170, 178, 184\}$ together with their symmetric ECA.

7.2 Study of trivial coalescence

The first step towards a complete classification of all ECA according to their coalescence behaviour is to identify trivial coalescence.

During our experimental study, we found that there are three possible ways to coalesce (see Figure 23): to a fixed point, before reaching a fixed point or to a configuration which is not a fixed point. The first one is not surprising, the second one is surprising when coalescence happens a long time before reaching a fixed point, and the third one is the most puzzling. For the second case, using different updating sequences would slow down coalescence and the “worst case” would be to coalesce once the fixed point is reached. Our qualitative exploration shows us that when coalescence happens on a configuration which is not a fixed point, this configuration completely depends on the updating sequence. Thus, we argue that ECA with no fixed points cannot have trivial coalescence.

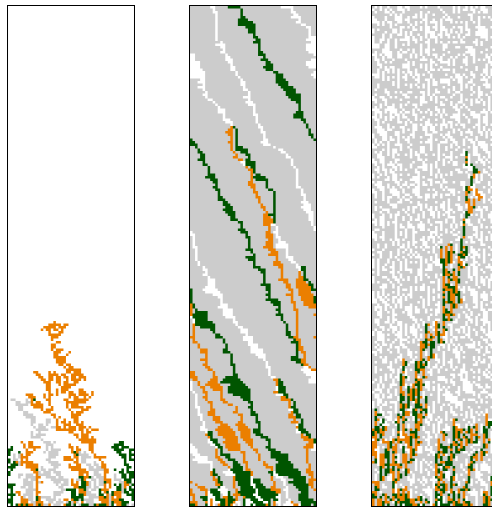


Figure 23: From left to right, agreement space-time diagrams of ECA 58, 154 and 62 with periodic boundary conditions and under fully asynchronous dynamics. ECA 58 coalesces once its only fixed point 0^n is reached (left); ECA 154, which has one reachable fixed point (0^n) and an unreachable one (1^n), coalesces a long time before reaching the fixed point (centre, full coalescence is not shown due to space constraints); and ECA 62 has a single fixed point which is unreachable, but it quickly coalesces to a non trivial configuration (right).

Next, we observe that all ECA having a set of fixed points $\mathcal{S} \not\subseteq \{0^n, 1^n\}$ cannot be trivial because their coalescence will depend on the ring size n .

Thus, we focus again in the set of ECA having a non empty set of fixed points $\mathcal{S} \subseteq \{0^n, 1^n\}$ is: $\{0, 2, 8, 10, 18, 24, 26, 32, 34, 38, 40, 42, 46, 50, 54, 56, 58, 60, 62, 106, 110, 122, 126, 128, 130, 136, 138, 146, 152, 154, 160, 162, 168, 170, 178, 184\}$. According to the number of fixed points and their reachability, we can classify them as follows:

- ECA with a single fixed point $\{0^n\}$ which is
 - Reachable: 0, 2, 8, 10, 18, 24, 26, 32, 34, 40, 42, 50, 56, 58, 106, and 122.

- Not reachable: 38, 46, 54, 60, 62, 110, and 126.
- ECA with two fixed points $\{0^n, 1^n\}$ of which
 - Both are reachable: 160, 162, 168, 170, 178, and 184.
 - One is reachable and the other one is unreachable: 128, 130, 136, 138, 146, 152, and 154.

Let us start analysing the subset of ECA with two fixed points. If both are reachable, then some configurations may evolve to one of them and some to the other one and thus lead to full disagreement. In particular, the evolutions of the ECA initialised at 0^n and initialised at 1^n could never coalesce. This is a non coalescent behaviour which could be formally described by using the definitions of coalescence with probability p (see Definition 5.5 on page 23). If one of the fixed points is reachable but not the other, we find again a non coalescent behaviour because we are sure that if the ECA is initialised at the unreachable fixed point, it will be unable to coalesce with the evolution of any other initial condition. Thus, this set of ECA is not trivial either. However, it would still be interesting to study their coalescence for the subset $\overline{\{1^n\}}$ of initial configurations (see Definition 5.3 on page 22).

If an ECA that only has one fixed point which is unreachable coalesces, it means that it coalesces in a configuration different from a fixed point and, as discussed above, this configuration will depend on the updating sequence. Thus, this subset of ECA cannot be trivial. Finally, if our classification of homogenising ECA is correct, then we can conclude that the set of ECA with trivial coalescence (i.e., both independent of the initial configuration and the sequence of updates, see Definition 5.2 on page 21) are the subset of ECA (conjectured homogenising) that have $\{0^n\}$ as only fixed point and it is reachable, that is, ECA 0, 2, 8, 10, 18, 24, 26, 32, 34, 40, 42, 50, 56, 58, 106, and 122. Most of them coalesce very quickly, i.e., in logarithmic time, few do it more slowly (they could take linear or quadratic time), and only ECA 122 does not coalesce quickly (we leave for future works the proof of its $WECT_{122}$ (see Definition 2.4 on page 11), which could be exponential or even infinite). However, these claims should be formally proven by finding lower and upper bounds to the coalescence time $t(n)$.

With all this information, we further claim that trivially coalescent ECA will coalesce in time $t(n) = WECT_f$ (see Definitions 2.4, 5.1 and 5.2).

7.3 Quadratic coalescence study

We have seen that coalescence may happen either if there is convergence to a fixed point or not. It is not very surprising when there is convergence to a fixed point and coalescence happens when this fixed point is reached. This kind of coalescent behaviour could be fully determined by studying the $WECT_f$ of these rules. However, we experimentally found that some ECA which are attracted to a (sometimes unreachable) fixed point coalesce a long time before this fixed point is reached, and this surprising behaviour cannot be fully determined by studying the $WECT_f$, because it will not correspond to the coalescence time.

Among the ECA presenting this kind of behaviour, we chose to study rule 154 (BCEG), which is doubly quiescent (see Definition 2.8 on page 14), because even though it takes a very long time to

reach a fixed point, its coalescence is rather fast. In particular, we would like to prove that it has a quadratic coalescence for any initial condition but the unreachable fixed point.

Using a de Bruijn diagram, it is easy to see that ECA 154 (BCEG) has only two fixed points: 0^n and 1^n . However, under fully asynchronous updates and starting from any configuration different from 1^n , only 0^n is reachable because an isolated zero could never disappear (D is not active).

7.3.1 Local behaviour analysis

We start by analysing how zones evolve in ECA 154. First of all, notice that any zero-zone having a size smaller than the ring size n limits with one-zones, and so it has a left frontier (10) and a right frontier (01), which we will respectively denote by L and R .

The active transitions of ECA 154 are B, C, E and G. From a detailed exploration of its letter code (see page 7), we can derive the following facts (see Figure 24):

- Since transitions A and H are not active, the number of zones cannot increase.
- The application of transitions B and C will increment the number of ones whilst the application of transitions E and G will increment the number of zeros.
- Since D is not active, an isolated zero cannot disappear. This implies that a zero-zone cannot disappear.
- The size of a zero-zone can evolve with the only constraint that it will bounce in case it has size one because D is not active.
- Since E is active, two zero-zones can merge once they are separated by only one zero. This implies that the number of zero-zones can decrease.
- Transitions B and C are only applicable if there is at least one zero-zones of size two or more. If so, transition B can be applied on its right boundary, and this would move R to the left and reduce the size of the zero-zone by one. Similarly, transition C can be applied on its left boundary, and this would move L to the right and reduce the size of the zero-zone by one.
- Transition G is only applicable where a zero-zone limits to its left-hand side with a one-zone of at least size two. If so, then the application of transition G would move L to the left and increase the size of the zero-zone by one.
- Since transition F is not active, a zero-zone cannot increment its size from the right-hand side frontier unless it merges from the right hand side with another zero-zone because transition E is applicable.

7.3.2 Global behaviour analysis

If we visualise the evolution of ECA 154 (see Figure 25) we see that the number of ones increases very quickly and zero-zones travel in average to the left forming streaks and merge when they meet.

This global behaviour can be explained from its local behaviour as follows:

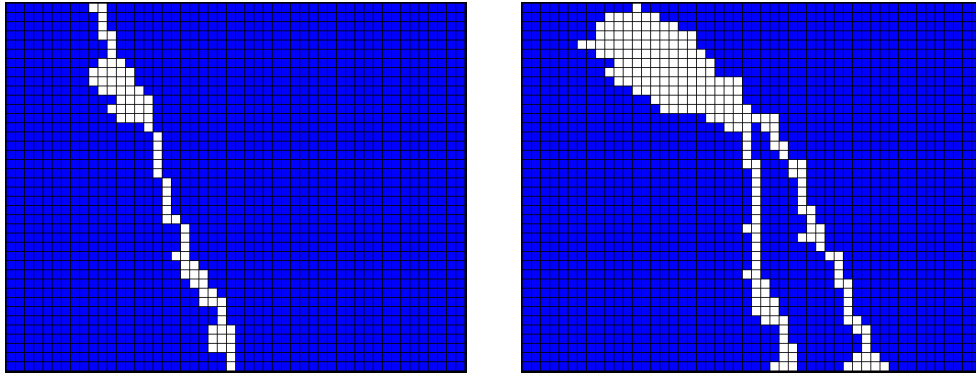


Figure 24: Space-time diagrams of ECA 154 with periodic boundary conditions and under fully asynchronous dynamics starting from an initial configuration with a single zero-zone (left) and starting from an initial configuration with two zero-zones (right).

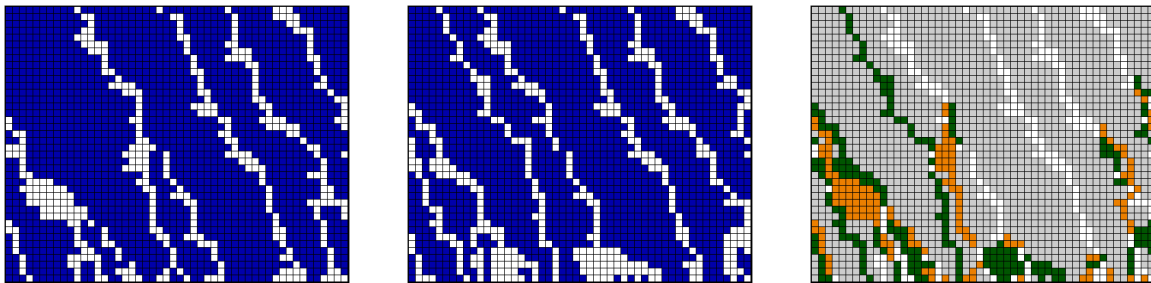


Figure 25: Evolution, from bottom to top, of ECA 154 with periodic boundary conditions following the same fully asynchronous updating sequence and starting from two different initial configurations (left and centre). Diagram with the superimposition of both CA showing their differences in green and orange and their agreement in white and grey (right).

- Zero-zones in ECA 154 tend to reduce their size (except when they have size one or when they merge with another zero-zone after applying transition E) because two active transitions (B and C) can reduce it and only one increase it (transition G). This implies that the number of ones increases in general.
- Zero-zones in ECA 154 travel in general to the left (except when they merge with another zero-zone after applying transition E) because the right boundary R can either remain or move to the left each time transition B is applied, and the left L boundary behaves as a random walk because transitions C and G act on it in opposite directions; i.e. each time that transition C is applied L moves to the right, and each time that transition G is applied L moves to the left.
- Zero-zones tend to merge because left boundaries travel faster than the right ones in average.

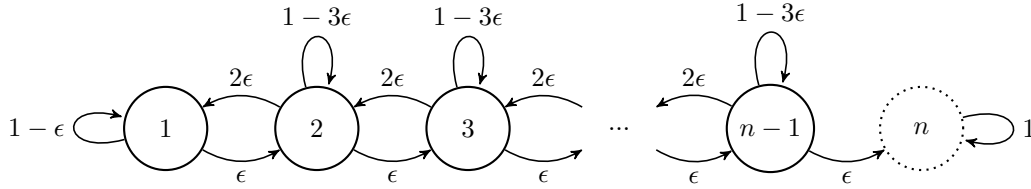
These observations will be formally proven in the following section by using Markov chains.

Remember that ECA 154 has a reachable fixed point 0^n and an unreachable fixed point 1^n . Hence, with the information we have so far we see that this ECA tends rather quickly to a configuration

with a single zero-zone, the size of which will behave as a random walk biased against the reachable fixed point. In particular, it can be shown that ECA 154 will eventually converge to 0^n with a $WECT_{154}$ in $\Theta(2^n)$ [17].

7.3.3 Mathematical analysis

We can analytically describe the evolution of the size of any zero-zone by means of the following Markov chain



where n is the ring size.

Thus, we see that zero-zones have a small size with high probability and that size one is a bouncing state. The state probabilities when n and t go to infinity can be found as follows:

Let $i \in \{1, \dots, n\}$ and $p_i^{(t)} = \mathbb{P}(X_t = i)$, where t is the time step and X_t a random variable taking values in $\{1, \dots, n\}$ representing the length a zero-zone can have. For $i \geq 2$,

$$p_i^{(t)} = (1 - 3\epsilon)p_i^{(t-1)} + 2\epsilon p_{i+1}^{(t-1)} + \epsilon p_{i-1}^{(t-1)}.$$

Thus, when t goes to infinity, we have:

$$\forall i \geq 2, \quad \lim_{t \rightarrow \infty} p_i^{(t)} = p_i = \frac{p_{i-1} + 2p_{i+1}}{3}.$$

For $i = 1$ we have that

$$p_1^{(t)} = (1 - \epsilon)p_1^{(t-1)} + 2\epsilon p_2^{(t-1)},$$

so that when t goes to infinity, $p_1 = 2p_2$. We can solve this recursive equation as follows:

$$x^2 - \frac{3}{2}x + \frac{1}{2} = (x - 1)(2x - 1) = 0$$

which has roots 1 and $\frac{1}{2}$, so

$$p_i = \alpha + \left(\frac{1}{2}\right)^i \beta.$$

Together with

$$p_1 = 2p_2$$

and knowing that

$$\sum_{i \geq 1} p_i = 1$$

we can deduce that $\alpha = 0$ and $\beta = 1$. Hence $p_i = \left(\frac{1}{2}\right)^i$ when n is large enough.

Studying the evolution of a single zero-zone, we see that if the probability of having length one (i.e. being in configuration $\mathbf{H}^{n-3}\mathbf{GDF}$) is p , then a zero-zone (actually, its left frontier 10) will move

to the left with an average speed v of $p\epsilon$, because **G** is the only active transition applicable in this situation. For any other size, the left frontier L will not move *in average* because both **C** and **G** will be equiprobably applicable and they move L in opposite directions. This can be formally written as follows: let Z_t be the random variable indicating the position of L and let $\Delta Z_{t+1} = Z_{t+1} - Z_t$. If $X_t = 1$ (state $\mathbf{H}^{n-3}\mathbf{GDF}$), then $\mathbb{E}[\Delta Z_{t+1} | x^t] = \epsilon$, else $\mathbb{E}[\Delta Z_{t+1} | x^t] = 0$. In particular, since we found that $p = \frac{1}{2}$ and taking $\epsilon = \frac{1}{n}$, $v = \frac{1}{2n}$. This can be illustrated with the experiment shown in Figure 26.

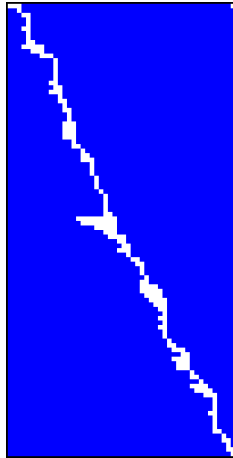


Figure 26: From bottom to top, evolution of fully asynchronous ECA 154 with ring size $n = 50$ starting from a configuration with a single zero (white cell) during 100 time steps. This example shows that, indeed, the zero-zone travels to the left with an average speed of $\frac{1}{2n} = \frac{1}{100}$.

According to these results, if we start from two zero-zones that are far apart and they both travel in the same direction (sense) and at the same *average* speed, they should in average never coalesce if there is no randomness. However, there is randomness in a fully asynchronous ECA because at each time step a cell is randomly and uniformly selected to be updated, i.e., it is a stochastic process. Thus, what we need to prove now is that these streaks moving to the left will merge.

We have seen that the left frontier L of a single zero-zone having size greater than one will not move in average. How is it possible, then, that we observe white streaks (zero-zones) moving rather quickly to the left? The answer is because, when a zero-zone has size greater than one, transition **B** is applicable on the right boundary R , it moves it to the left and reduces the size of the zero-zone by one; and we have already proved that size one is the most probable state in the Markov chain representing the size evolution of a zero-zone.

We experimentally observe that all zero-zones merge until only one is left, and ECA 154 coalescence usually takes place when the two single zero-zones of each copy coincide. Thus, studying the merging of two zero-zones we will be able to characterise the global behaviour of this ECA and bound its coalescence time.

Our hypothesis is that ECA 154 coalesces in $\Theta(n^2)$, i.e., quadratic time. In order to formally prove this claim we would have to provide quadratic lower and upper bounds. This is quite difficult,

especially because any claim or general property about an ECA has to be proven for any ring size and any possible initial condition. This is a computationally untreatable figure without a proper previous formal study which reduces the number of study cases. In what follows, we will provide a lower bound and a particular case of upper bound.

Lower bound

Two copies of ECA 154 following the same fully asynchronous sequence of updates and starting from an initial configuration with a single zero-zone will not be able to coalesce before these two possibly disagreeing zones meet in the agreement space-time diagram; i.e. the two zero-zones reach the same position at the same time (see Figure 27). Thus, a lower bound to ECA 154 coalescence time will be given by the expected time that it takes for two separate zero-zones to meet.

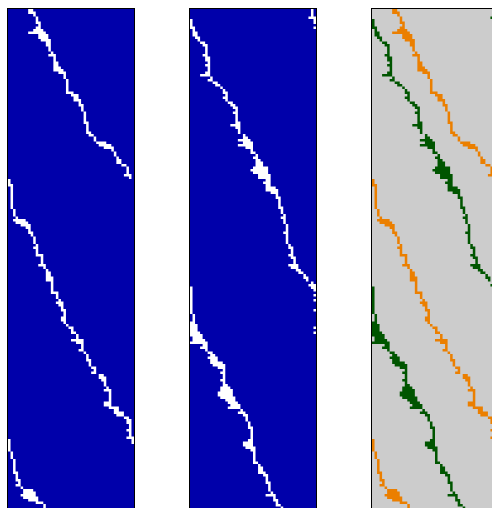


Figure 27: Two space-time diagrams of ECA 154 with periodic boundary conditions following the same fully asynchronous sequence of updates and starting from a single 0 (left and centre). The agreement space-time diagram illustrates that coalescence is not possible before the two zero-zones meet (right).

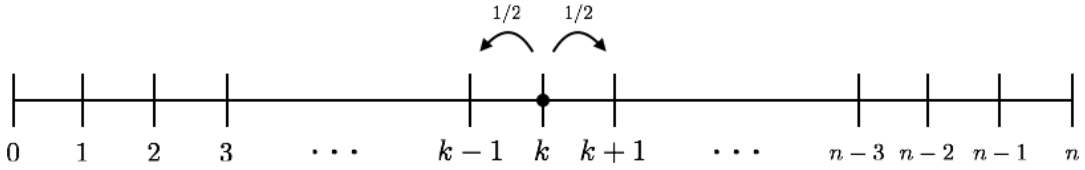
Let n be the ring size and $k \in \{0, \dots, n\}$ be the distance between two zero-zones. Since we have periodic boundary conditions, we take the distance that goes from one zero-zone to the other without crossing any ring boundary. Thus, we will first only be concerned about the right boundary of the zero-zone in the left hand side position and with the left boundary of the zero-zone in the right hand side. Later we will see that we can treat the zero-zones as points on a line without loss of generality.

From the previous analysis we know that a zero-zone will have, *in average*, size one with probability $\frac{1}{2}$, and so it will have a size bigger than one with probability $\frac{1}{2}$. Thus, we have:

- With probability $\frac{1}{4}$ both zero-zones will have size one. In this situation, only transition G applied in the right hand side zero-zone will modify the distance between zero-zones. Hence, k will be reduced by one with probability $\frac{1}{n}$.

- With probability $\frac{1}{4}$ both zero-zones will have size greater than one. In this situation we will go to $k - 1$ with probability $\frac{1}{n}$ (because of transition G possible application in the right hand side zero-zone) and to $k + 1$ with probability $\frac{2}{n}$ (because of transition C possible application in the right hand side zero-zone and transition B possible application in the left hand side zero-zone).
- With probability $\frac{1}{4}$ the zero-zone in the left hand side will have size one and the other one will have size greater than one. In this situation, only transition C and G applied in the right hand side zero-zone will modify the distance between zero-zones. In particular, we will obtain $k + 1$ with probability $\frac{1}{n}$ and $k - 1$ with probability $\frac{1}{n}$.
- With probability $\frac{1}{4}$ the zero-zone in the left hand side will have size greater than one and the other one will have size one. In this situation, only transition B applied in the left hand side zero-zone and G applied in the right hand side zero-zone will modify the distance between zero-zones. In particular, we will obtain $k + 1$ with probability $\frac{1}{n}$ and $k - 1$ with probability $\frac{1}{n}$.

Hence we have that the distance between two zero-zones will increase by one with probability $\frac{1}{4} \frac{1}{n}$ and will decrease by one with probability $\frac{1}{4} \frac{1}{n}$. We conclude that, in average, it has the same probability to increase than to decrease. Thus, the distance k behaves as an unbiased random walk and, without loss of generality, we can study it as follows:



Since we are in a ring, there are two possibilities that two zero-zones can meet: if the right one catches the left one or if the left one catches the right one (by crossing the boundary and becoming the zero-zone in the right). Let T_k be the expected time to reach 0 or n from position k . Then

$$\mathbb{E}[T_k] = \frac{1}{2}\mathbb{E}[T_{k-1}] + \frac{1}{2}\mathbb{E}[T_{k+1}] + 1,$$

which rewritten in the form of a recursive equation becomes

$$l_k = \frac{l_{k-1}}{2} + \frac{l_{k+1}}{2} + 1,$$

that has solution

$$l_k = -k^2 + \alpha k + \beta.$$

Knowing that $l(0) = l(n) = 0$, we can deduce that $\alpha = n$ and $\beta = 0$, so that

$$l_k = k(n - k).$$

Thus, $\max_k \mathbb{E}[T_k] = \frac{n}{2}(n - \frac{n}{2}) = \frac{n^2}{4}$, because $k = \frac{n}{2}$ is the maximum distance to both 0 and n .

From the definition of coalescence, we have that

$$t(n) = \max_{x,y} \mathbb{E}[T_{xy}] \geq \mathbb{E}[T_{xy}] \text{ for all } x, y \in Q^U.$$

Thus $t(n) \geq l \iff \exists x, y$ such that $\mathbb{E}[T_{xy}] \geq l$. This means that finding a particular lower bound for $\mathbb{E}[T_{xy}]$ gives us a general lower bound for $t(n)$. Notice that in order to avoid trivial lower bounds such as $t(n) > 0$, we would like to find sharp or tight bounds (see Definition 6.2 on page 26).

We discussed above that coalescence cannot happen before the two last zero-zones (in different copies) meet, and we found that this meeting time is bounded by n^2 . Thus, we can say that ECA 154 coalescence time $t(n) \geq n^2$ has a quadratic lower bound; i.e. $t(n) = \Omega(n^2)$.

Particular upper bound

Let K_t be the random variable taking values in $\{0, \dots, n\}$ representing the distance between two zero-zones, let $\Delta K_t = K_t - K_{t-1}$, and let $(\mathcal{K}_t)_{t \in \mathbb{N}}$ be the sequence of past values taken by K_t up to t . Then, with the previous study it is clear that $(K_t)_{t \in \mathbb{N}}$ is a sequence of random variables of *type I* (see Definition 6.1 on page 25) because $\mathbb{E}[\Delta K_t \mid \mathcal{K}_t] = \frac{1}{4n} - \frac{1}{4n} = 0$, so (K_t) is a martingale, and if $0 < K_t < n$, then $P(\Delta K_{t+1} \geq 1 \mid \mathcal{K}_t) = P(\Delta K_{t+1} \leq -1 \mid \mathcal{K}_t) = \epsilon = \frac{1}{4n}$. Thus, we can apply Lemma 6.2 (see page 25) and obtain

$$\mathbb{E}[T_k] \leq \frac{k_0(n - k_0)}{2\epsilon} = 2n^2 k_0 - 2nk_0^2 = 2nk_0(n - k_0)$$

where k_0 is the initial distance between two zero-zones.

This gives us a particular quadratic upper bound for $\mathbb{E}[T_{xy}]$, but it is not a general upper bound for $t(n)$ because

$$\exists x, y : \mathbb{E}[T_{xy}] \leq u \not\Rightarrow t(n) \leq u.$$

7.4 Linear coalescence study

In this section we choose to study one of the most surprising coalescent behaviours, namely when an ECA coalesces very quickly to a configuration which is not a fixed point. From the ECA presenting this kind of behaviour, we choose to study rule 62 (BCDGH). We conjecture that ECA 62 (and also ECA 38 and ECA 46 which present a similar behaviour) coalesces in linear time (see Figure 28).



Figure 28: Evolution, from bottom to top, of ECA 62 with periodic boundary conditions following the same fully asynchronous updating sequence and starting from two different initial configurations (left and centre). Diagram with the superimposition of both CA showing their differences in green and orange and their agreement in white and grey (right).

Using a de Bruijn diagram, it is easy to see that ECA 62 (BCDGH) has only one fixed point 0^n . However, under fully asynchronous dynamics and starting from any configuration different from 0^n , this fixed point is unreachable because an isolated one could never disappear (E is not active).

Lower bound

After performing a similar qualitative study and mathematical analysis than the one we realised in the previous section for ECA 154 (see Figure 29), we deduce that, if each copy has a single one-zone, coalescence cannot happen before these one-zones meet.

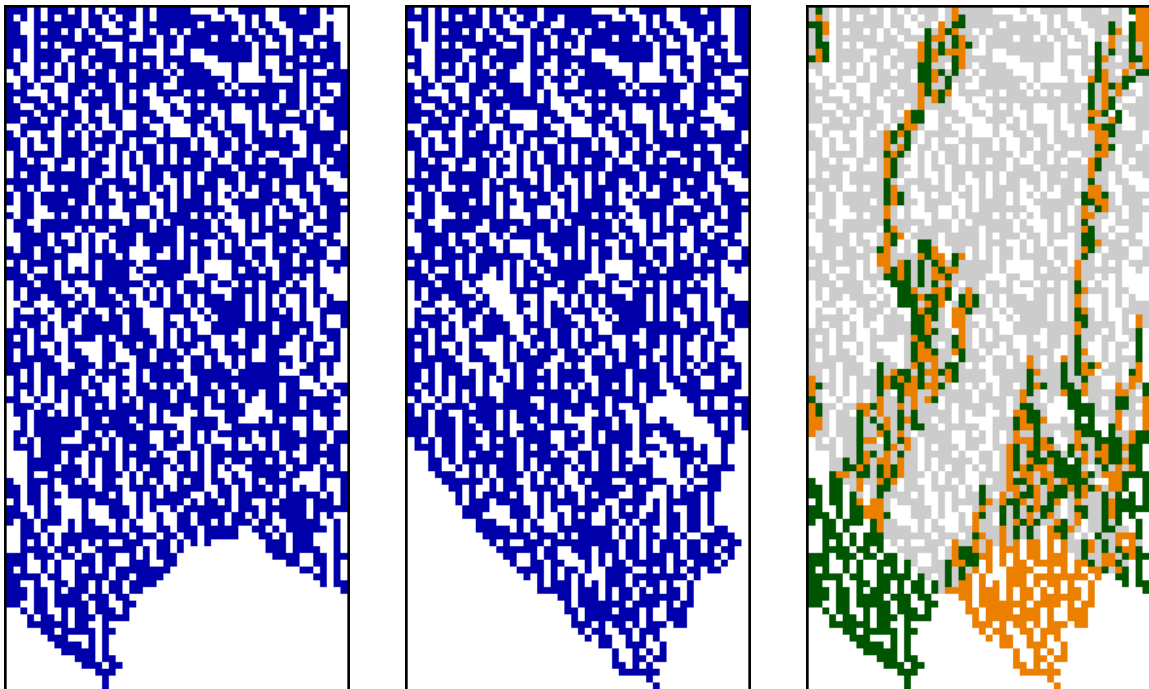


Figure 29: Two space-time diagrams of ECA 62 with periodic boundary conditions following the same fully asynchronous sequence of updates and starting from a single 1 (left and centre). Agreement space-time diagram showing that coalescence is not possible before the boundaries of the two original one-zones meet (right).

Let k be the distance between two one-zones. Then the furthest apart that they can be from each other is $\frac{n}{2}$ (because we have periodic boundary conditions). Then, to go from $k = \frac{n}{2}$ to $k = 0$ (i.e., the two one-zones meet), we need *in average* at least $\frac{n}{4}$ time steps. This gives us a linear lower bound, because

$$t(n) \geq \mathbb{E}[T_{xy}] \geq \frac{n}{4}.$$

Upper bound

In order to find a linear upper bound, we would like to construct an always-decreasing energy function for any ring size and any initial configuration and apply Lemma 6.1 to it (see page 25). We studied all possible transitions in all possible neighbourhoods of size 5 and created a Java program in order to test our hypothesis. However, we could not find yet an always decreasing energy function that would allow us to apply Lemma 6.1 and give proof of the existence of a linear upper bound.

8 Conclusion

We have defined and studied cellular automata (CA). From their general definition we focused on the study of elementary cellular automata (ECA) with periodic boundary conditions. We studied their basic properties and saw that the total of 256 ECA can be reduced to 88 equivalence classes. We were able to visualise their global behaviour by plotting their space-time diagram using FiatLux software. We discussed different updating schemes, namely synchronous, partially asynchronous and fully asynchronous and their influence in the dynamics of a CA. Then we informally defined the concept of coalescence and extended FiatLux in order to plot what we called agreement space-time diagram, which is the superimposition of two space-time diagrams showing the difference between them.

With this tool we performed an extensive qualitative exploration of the coalescent behaviour of the 88 minimal representatives of all ECA under fully asynchronous dynamics. From this experimental exploration we distinguished several different kinds of coalescence styles (e.g. trivial, for a subset of configurations, etc.), which we later fully characterised after formally defining coalescence.

The general goal of this project was to give the first steps towards a global classification of all ECA according to their coalescence behaviour. We did a first rough classification based on our experimental study, but conjectures need to be formally proven. However, this is a difficult task because all claims need to be proven for any ECA size and any possible initial configuration. After more than 40 years of study and lots of effort, it is still difficult for the community to even classify the set of synchronous ECA, which are deterministic and the simplest kind of CA. This clearly shows the hidden complexity of this kind of discrete systems. We are very far from reaching a complete characterisation of this new CA property, but maybe the study of new and old ECA features will allow us to understand them or at least provide a full taxonomy.

Nevertheless, we started the analytical study of coalescence in fully asynchronous ECA and were able to give some formal proofs. In particular, we analytically studied trivial coalescence and conjectured that the only fully asynchronous ECA that could have this kind of coalescence (independent of both the initial condition and the sequence of updates) are ECA 0, 2, 8, 10, 18, 24, 26, 32, 34, 40, 42, 50, 56, 58, 106, and 122.

We conjectured that ECA 154 coalesces in quadratic time for any initial configuration different from 1^n and began the formal proof of this statement by finding a quadratic lower bound and a particular upper bound. We also conjectured that ECA 62 coalesces in linear time and began the formal proof of this claim by finding a linear lower bound and suggesting an analytical way to find a linear upper bound in order to prove the conjecture. In particular, we propose to find an always-decreasing energy function (this can be tested for any size and configuration using our Java code) to be able to apply a mathematical result that would give us a linear upper bound for any size and any initial configuration.

These results have been obtained after a four-months research internship. They are still partial and might seem limited, but these are some of the first steps in the study of coalescence. We should keep working in order to further understand cellular automata and their significance.

Acknowledgements

I would like to thank both of my supervisors for their guidance, encouragement and advice. They have both been very attentive and helpful.

References

- [1] M. S. Alber, M. A. Kiskowski, J. A. Glazier, and Y. Jiang. On cellular automaton approaches to modeling biological cells. pages 1–39, 2003.
- [2] M. Bartolozzi and A. W. Thomas. Stochastic cellular automata model for stock market dynamics. *Physical review E*, 69(4):046112, 2004.
- [3] L. Bartosik, J. Stafiej, and D. Di Caprio. Cellular automata model of anodization. *Journal of Computational Science*, 11:309–316, 2015.
- [4] E. Berlekamp, J. Conway, and R. Guy. Winning ways for your mathematical plays academic. *New York*, 2, 1982.
- [5] A. Bušić, N. Fatès, J. Mairesse, and I. Marcovici. Density classification on infinite lattices and trees. *Electron. J. Probab*, 18(51):1–22, 2013.
- [6] A. Bušić, J. Mairesse, and I. Marcovici. Probabilistic cellular automata, invariant measures, and perfect sampling. *Advances in Applied Probability*, 45(04):960–980, 2013.
- [7] M. Cook. Universality in elementary cellular automata. *Complex Systems*, 15:1–40, 2004.
- [8] S. Coombes. The geometry and pigmentation of seashells. *Techn. Ber. Department of Mathematical Sciences*, 2009.
- [9] A. Deutsch. Principles of biological pattern formation: swarming and aggregation viewed as selforganization phenomena. *Journal of biosciences*, 24(1):115–120, 1999.
- [10] A. Deutsch and S. Dormann. *Cellular automaton modeling of biological pattern formation: characterization, applications, and analysis*. Springer Science & Business Media, 2007.
- [11] G. Engelen, R. White, I. Uljee, and P. Drazan. Using cellular automata for integrated modelling of socio-environmental systems. *Environmental monitoring and Assessment*, 34(2):203–214, 1995.
- [12] J. M. Epstein. Agent-based computational models and generative social science. *Complexity*, 4(5):41–60, 1999.
- [13] N. Fatès. Directed percolation phenomena in asynchronous elementary cellular automata. In S. El Yacoubi, B. Chopard, and S. Bandini, editors, *Proceedings of the 7th ACRI conference*, volume 4173 of *LNCS*, pages 667–675. Springer, 2006.
- [14] N. Fatès. A guided tour of asynchronous cellular automata. *Journal of Cellular Automata*, 9(5-6):387–416, 2014.
- [15] N. Fatès. Remarks on the cellular automaton global synchronisation problem. In J. Kari, editor, *Proceedings of AUTOMATA 2015*, volume 9099 of *Lecture Notes in Computer Science*, pages 113–126. Springer, 2015. doi: 10.1007/978-3-662-47221-7_

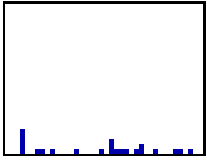
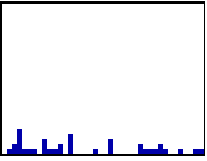
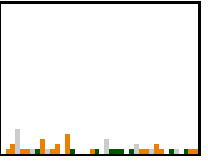
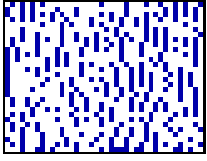
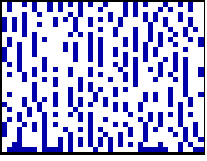
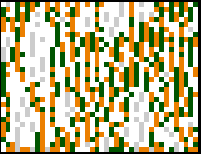
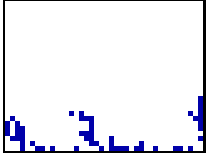
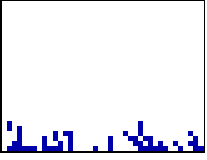
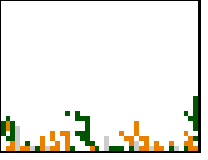


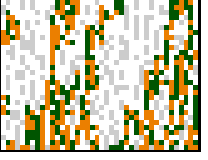
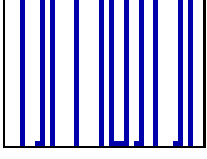
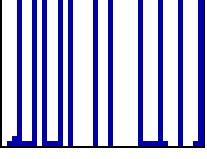
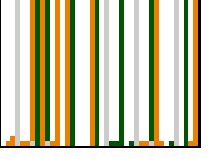
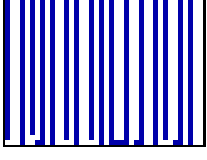
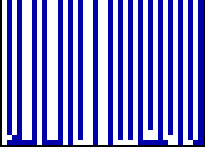
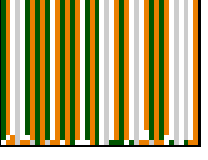
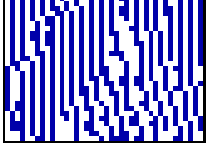
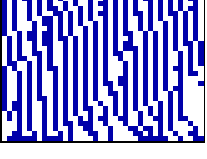
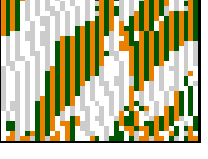
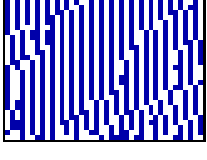
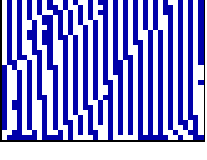
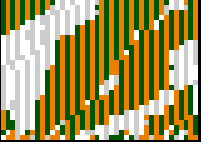
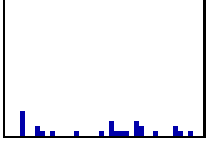
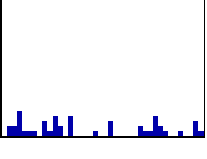
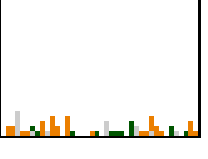
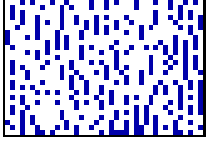

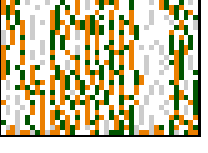
9. extended version available on <https://members.loria.fr/nazim.fates/dwnld/submitted-GlobalSynchProblem-Fates17.pdf>.
- [16] N. Fatès and M. Morvan. An experimental study of robustness to asynchronism for elementary cellular automata. *Complex Systems*, 16:1–27, 2005.
- [17] N. Fatès, M. Morvan, N. Schabanel, and E. Thierry. Fully asynchronous behavior of double-quiescent elementary cellular automata. *Theoretical Computer Science*, 362:1–16, 2006. doi: 10.1016/j.tcs.2006.05.036.
- [18] N. Fatès, I. Marcovici, and S. Taati. Two-dimensional traffic rules and the density classification problem. In *International Workshop on Cellular Automata and Discrete Complex Systems*, pages 135–148. Springer, 2016.
- [19] M. Gardner. Mathematical games: The fantastic combinations of john conways new solitaire game life. *Scientific American*, 223(4):120–123, 1970.
- [20] D. Green. Cellular automata models in biology. *Mathematical and Computer Modelling*, 13(6): 69–74, 1990.
- [21] J. Kari. The nilpotency problem of one-dimensional cellular automata. *siam Journal on Computing*, 21(3):571–586, 1992.
- [22] I. Kusch and M. Markus. Mollusc shell pigmentation: cellular automaton simulations and evidence for undecidability. *Journal of theoretical biology*, 178(3):333–340, 1996.
- [23] J. Lee, S. Adachi, F. Peper, and K. Morita. Asynchronous game of life. *Physica D*, 194(3–4): 369–384, 2004. doi: 10.1016/j.physd.2004.03.007.
- [24] T. Liggett. *Interacting particle systems. classics in mathematics (reprint of first edition)*, 2005.
- [25] R. Lipton, R. Miller, and L. Snyder. Synchronization and computing capabilities of linear asynchronous structures. *Journal of Computer and System Sciences*, 14(1):49–72, 1977. doi: 10.1016/S0022-0000(77)80040-8.
- [26] M. Macauley and H. S. Mortveit. Coxeter groups and asynchronous cellular automata. In S. Bandini, S. Manzoni, H. Umeo, and G. Vizzari, editors, *Proceedings of ACRI'10*, volume 6350 of *Lecture Notes in Computer Science*, pages 409–418. Springer, 2010. doi: 10.1007/978-3-642-15979-4_43.
- [27] M. Macauley, J. McCammond, and H. S. Mortveit. Order independence in asynchronous cellular automata. *Journal of Cellular Automata*, 3(1):37–56, 2008. URL <http://www.oldcitypublishing.com/JCA/JCAabstracts/JCA3.1abstracts/JCAv3n1p37-56Macauley.html>.
- [28] M. Macauley, J. McCammond, and H. Mortveit. Dynamics groups of asynchronous cellular automata. *Journal of Algebraic Combinatorics*, 33(1):11–35, 2011. doi: 10.1007/s10801-010-0231-y.

- [29] J. Mairesse and I. Marcovici. Around probabilistic cellular automata. *Theoretical Computer Science*, 559(0):42–72, 2014. doi: 10.1016/j.tcs.2014.09.009. Non-uniform Cellular Automata.
- [30] L. Manukyan, S. A. Montandon, A. Fofonjka, S. Smirnov, and M. C. Milinkovitch. A living mesoscopic cellular automaton made of skin scales. *Nature*, 544(7649):173–179, 2017.
- [31] O. Martin, A. M. Odlyzko, and S. Wolfram. Algebraic properties of cellular automata. *Communications in Mathematical Physics*, 93:219, 1984.
- [32] K. Nakamura. Asynchronous cellular automata and their computational ability. *Systems, Computers, Controls*, 5(5):58–66, 1974.
- [33] K. Nakamura. Synchronous to asynchronous transformation of polyautomata. *Journal of Computer and System Sciences*, 23(1):22 – 37, 1981. doi: [http://dx.doi.org/10.1016/0022-0000\(81\)90003-9](http://dx.doi.org/10.1016/0022-0000(81)90003-9). URL <http://www.sciencedirect.com/science/article/pii/0022000081900039>.
- [34] C. L. Nehaniv. Asynchronous automata networks can emulate any synchronous automata network. *International Journal of Algebra and Computation*, 14(5-6):719–739, 2004. doi: 10.1142/S0218196704002043.
- [35] A. Nowak and M. Lewenstein. Modeling social change with cellular automata. In *Modelling and simulation in the social sciences from the philosophy of science point of view*, pages 249–285. Springer, 1996.
- [36] F. Peper, T. Isokawa, N. Kouda, and N. Matsui. Self-timed cellular automata and their computational ability. *Future Generation Computer Systems*, 18(7):893–904, 2002. doi: 10.1016/S0167-739X(02)00069-9.
- [37] F. Peper, S. Adachi, and J. Lee. Variations on the game of life. In A. Adamatzky, editor, *Game of Life Cellular Automata*, pages 235–255. Springer London, 2010. doi: 10.1007/978-1-84996-217-9_13.
- [38] J.-B. Rouquier. *Robustesse et mergence dans les systmes complexes: le modle des automates cellulaires*. PhD thesis, cole Normale Suprieure de Lyon, December 2008. URL <http://rouquier.org/jb/recherche/these.php>.
- [39] J.-B. Rouquier. An exhaustive experimental study of synchronization by forcing on elementary cellular automata. In B. Durand, editor, *Proceedings of the First Symposium on Cellular Automata*, pages 250–261. MCCME Publishing House, Moscow, April 2008. ISBN 978-5-94057-377-7. URL <http://hal.archives-ouvertes.fr/hal-00274006/en/>.
- [40] J.-B. Rouquier and M. Morvan. Coalescing cellular automata. In V. N. Alexandrov, G. D. van Albada, P. M. A. Sloot, and J. Dongarra, editors, *Proceedings of the 6th International Conference on Computational Science (ICCS)*, volume 3993 of *Lectures Notes in Computer Science*, pages 321–328. Springer Berlin, May 2006. ISBN 3-540-34383-0. doi: 10.1007/11758532_44. URL <http://prunel.ccsd.cnrs.fr/ensl-00103510/fr/>.

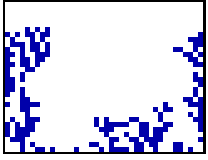
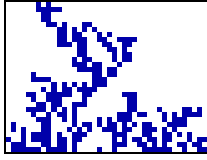
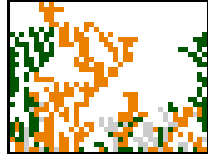


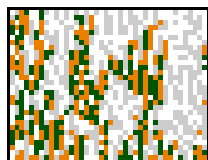
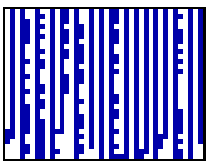
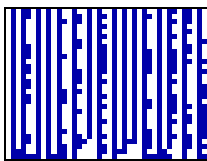

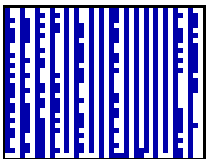
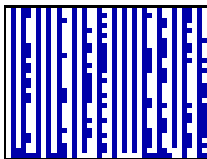

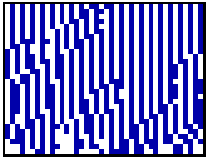
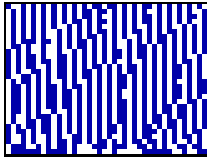
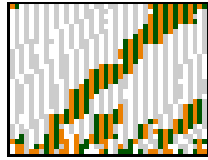
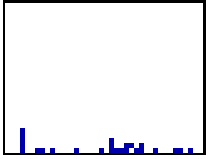
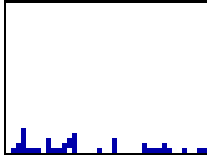
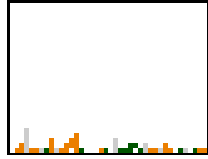


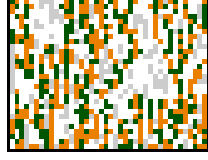
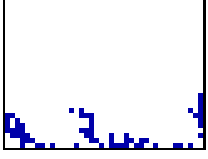
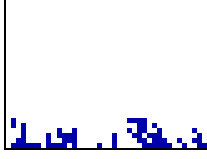
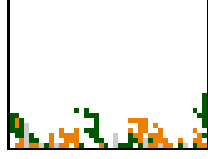


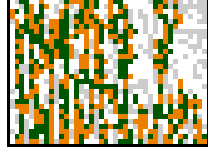
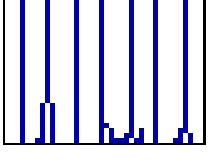
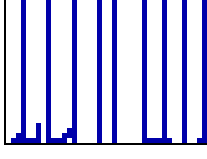
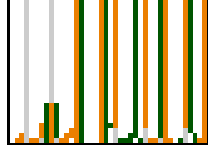
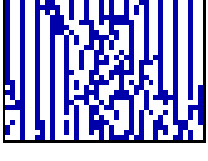
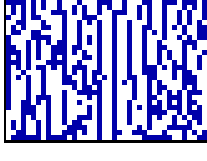
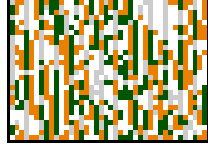

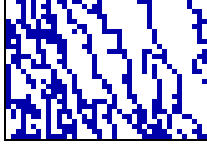
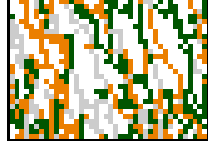
- [41] J.-B. Rouquier and M. Morvan. Combined effect of topology and synchronism perturbation on cellular automata: Preliminary results. In H. Umeo, S. Morishita, and K. Nishinari, editors, *ACRI*, volume 5191 of *LNCS*. Springer Berlin, 2008. doi: 10.1007/978-3-540-79992-4_28. URL http://www.rouquier.org/jb/research/papers/2008_topology_perturbation/topology_perturbation.pdf.
- [42] J.-B. Rouquier and M. Morvan. Coalescing cellular automata: Synchronization by common random source for asynchronous updating. *Journal of Cellular Automata*, 4(1):55–78, 2009. URL <http://www.oldcitypublishing.com/JCA/JCAabstracts/JCA4.1abstracts/JCAv4n1p55-77Rouquier.html>.
- [43] J. B. Salem and S. Wolfram. Thermodynamics and hydrodynamics with cellular automata. *Phys. Rev. Lett.*, 1985.
- [44] J. Von Neumann. The general and logical theory of automata. *Cerebral mechanisms in behavior*, 1(41):1–2, 1951.
- [45] J. von Neumann. *Theory of self-reproducing automata*. University of Illinois press Urbana, 1966. A. Burks (editor).
- [46] L. Wang, X. Wang, and J. Wang. Limit set problem of multi-agent systems with finite states: An eigenvalue-based approach. *Journal of Systems Science and Complexity*, 28(3):570–579, 2015.
- [47] R. White and G. Engelen. Cellular automata and fractal urban form: a cellular modelling approach to the evolution of urban land-use patterns. *Environment and planning A*, 25(8):1175–1199, 1993.
- [48] S. Wolfram. Computation theory of cellular automata. *Communications in mathematical physics*, 96(1):15–57, 1984.
- [49] S. Wolfram. *Cellular automata and complexity: collected papers*, volume 1. Addison-Wesley Reading, MA, 1994.
- [50] S. Wolfram. *A new kind of science*. Wolfram Media Inc., 2002.
- [51] T. Worsch. Towards intrinsically universal asynchronous CA. *Natural Computing*, 12(4):539–550, 2013. doi: 10.1007/s11047-013-9388-3. URL <https://doi.org/10.1007/s11047-013-9388-3>.

A Taxonomy table

Table 5: Each row corresponds to one of the 88 minimal representatives ECA. Their Wolfram's code is given in the first column, together with the code of the rest of ECA belonging to the same class. The second column contains Fatès' letter code for the minimal representative. The third column gives the set of fixed points of the minimal representative. Conjectures about the coalescent behaviour of each of the 88 ECA are given in the fourth column. Notice that this classification is experimental-based and provisional until it is formally proven. Columns five, six and seven give visual examples of the global behaviour and coalescence style of each minimal ECA. If needed, some comments are given in the rightmost column.

Wolfram's code	Fatès' code	Fixed points	Coalescence style	Space-time diagram I	Space-time diagram II	Agreement space-time diagram of I and II	Comments
0 (255)	EFGH	0^n	Trivial in $t(\log n)$				
1 (127)	A EFGH	-	-				Study evolution of coalescence percentage and its average
2 (16, 191, 247)	B EFGH	0^n	Trivial in $t(\log n)$				
3 (17, 63, 119)	A B EFGH	-	To a non-trivial configuration in $t(n)$				
4 (223)	F GH	0^n (unreachable), $(01)^n$, $(CA^i BE(DE)^j)^k$	-				
5 (95)	A F GH	$(01)^n$, $(CBE(DE)^i)^j$	-				
6 (20, 159, 215)	B F GH	0^n (unreachable), $(01)^n$	Shift coalescence in $t(n^2)$				May coalesce before reaching the fixed point
7 (21, 31, 87)	A B F GH	$(01)^n$	Shift coalescence in $t(n^2)$				May coalesce before reaching the fixed point
8 (64, 239, 253)	E GH	0^n	Trivial in $t(\log n)$				
9 (65, 111, 125)	A E GH	-	-				Study evolution of coalescence percentage and its average

Wolfram's code	Fatès' code	Fixed points	Coalescence style	Space-time diagram I	Space-time diagram II	Agreement space-time diagram of I and II	Comments
10 (80, 175, 245)	BEGH	0^n	Trivial in $t(\log n)$				
11 (81, 47, 117)	ABEGH	-	To a non-trivial configuration in $t(n)$				
12 (68, 207, 221)	GH	0^n (unreachable), $(01)^n$, $(CA^i BE(DE)^j)^k$	-				
13 (69, 79, 93)	AGH	$(01)^n$, $(CBE(DE)^i)^j$	-				
14 (84, 143, 213)	BGH	0^n (unreachable), $(01)^n$	Shift coalescence in $t(n^2)$				May coalesce before reaching the fixed point
15 (85)	ABGH	$(01)^n$	Shift coalescence in $t(n)$				May coalesce before reaching the fixed point
18 (183)	BCEFGH	0^n	Trivial in $t(\log n)$				
19 (55)	ABCEFGH	-	To a non-trivial configuration in $t(n^2)$				
22 (151)	BCFGH	0^n (unreachable), $(01)^n$	Shift coalescence in $t(n)$				May coalesce before reaching the fixed point
23	ABCFGH	$(01)^n$	Shift coalescence in $t(n)$				May coalesce before reaching the fixed point
24 (66, 231, 189)	CEGH	0^n	Trivial in $t(\log n)$				
25 (67, 103, 61)	ACEGH	-	-				Study evolution of coalescence percentage and its average

Wolfram's code	Fatès' code	Fixed points	Coalescence style	Space-time diagram I	Space-time diagram II	Agreement space-time diagram of I and II	Comments
26 (82, 167, 181)	BCEGH	0^n	Trivial in $t(\log n)$				
27 (83, 39, 53)	ABCEGH	-	To a non-trivial configuration in $t(n)$				
28 (70, 199, 157)	CGH	0^n (unreachable), $(01)^n$	-				
29 (71, 29)	ACGH	$(01)^n$	-				
30 (86, 135, 149)	BCGH	0^n (unreachable), $(01)^n$	Shift coalescence in $t(n^2)$				May coalesce before reaching the fixed point
32 (251)	DEFGH	0^n	Trivial in $t(\log n)$				
33 (123)	ADEFGH	-	-				May coalesce because of periodic boundary conditions
34 (48, 187, 243)	BDEFGH	0^n	Trivial in $t(\log n)$				
35 (49, 59, 115)	ABDEFGH	-	To a non-trivial configuration in $t(n)$				
36 (219)	DFGH	0^n (unreachable), $(CA^i BE)^j$	-				
37 (91)	ADFGH	$(CBE)^i$	-				May coalesce because of periodic boundary conditions
38 (52, 155, 211)	BDFGH	0^n (unreachable)	To a non-trivial configuration in $t(n)$				

Wolfram's code	Fatès' code	Fixed points	Coalescence style	Space-time diagram I	Space-time diagram II	Agreement space-time diagram of I and II	Comments
40 (96, 235, 249)	DEGH	0^n	Trivial in $t(\log n)$				
41 (97, 107, 121)	ADEGH	-	-				Study evolution of coalescence percentage and its average
42 (112, 171, 241)	BDEGH	0^n	Trivial in $t(\log n)$				
43 (113)	ABDEGH	-	To a non-trivial configuration with probability p				May reach full disagreement on a non-trivial configuration
44 (100, 203, 217)	DGH	0^n (unreachable), $(CA^i BE)^j$	-				
45 (101, 75, 89)	ADGH	$(CBE)^i$	-				May coalesce because of periodic boundary conditions
46 (116, 139, 209)	BDGH	0^n (unreachable)	To a non-trivial configuration in $t(n)$				
50 (179)	BCDEFGH	0^n	Trivial in $t(\log n)$				
51	ABCDEFGH	-	-				Disagreements in the initial configuration will remain
54 (147)	BCDFGH	0^n (unreachable)	-				Study evolution of coalescence percentage and its average
56 (98, 227, 185)	CDEGH	0^n	Trivial in $t(\log n)$				
57 (99)	ACDEGH	-	-				Study evolution of coalescence percentage and its average

Wolfram's code	Fatès' code	Fixed points	Coalescence style	Space-time diagram I	Space-time diagram II	Agreement space-time diagram of I and II	Comments
58 (114, 163, 177)	BCDEGH	0^n	Trivial in $t(\log n)$				
60 (102, 195, 153)	CDGH	0^n (unreachable)	-				
62 (118, 131, 145)	BCDGH	0^n (unreachable)	To a non-trivial configuration in $t(n)$				
72 (237)	EH	0^n , DFG, $(CA^i BFG(DFG)^j)^k$	-				
73 (109)	AEH	DFG, $(CBFG(DFG)^i)^j$	-				
74 (88, 173, 229)	BEH	0^n , $(DFG)^i$	With probability p , and shift-coalescent with probability $1-p$				Could be trivial in $t(n)$ for a subset of configurations
76 (205)	H	All configurations except 1^n	-				
77	AH	All configurations except 0^n and 1^n	-				
78 (92, 141, 197)	BH	0^n (unreachable), $(01)^n$, $(FGD(ED)^i)^j$	-				
90 (165)	BCEH	0^n , $(DFG)^i$	-				
94 (133)	BCH	0^n (unreachable), $(01)^n$, $(FGD(ED)^i)^j$	-				
104 (233)	DEH	0^n , $(CA^i BFG)^j$	-				

Wolfram's code	Fatès' code	Fixed points	Coalescence style	Space-time diagram I	Space-time diagram II	Agreement space-time diagram of I and II	Comments
105	ADEH	$(CBFG)^i$	-				Study evolution of coalescence percentage and its average
106 (120, 169, 225)	BDEH	0^n	Trivial in $t(n)$				
108 (201)	DH	0^n (unreachable), $(CA^i BE)^j$, $(CA^k BFGC)^l$	-				
110 (124, 137, 193)	BDH	0^n (unreachable)	-				Study evolution of coalescence percentage and its average
122 (161)	BCDEH	0^n	Trivial in $t(2^n)$?				Prove first its <i>WECT</i>
126 (129)	BCDH	0^n (unreachable)	-				Study evolution of coalescence percentage and its average
128 (254)	EFG	0^n , 1^n (unreachable)	Trivial in $t(\log n)$ except for configuration 1^n				
130 (144, 190, 246)	BEFG	0^n , 1^n (unreachable)	Trivial in $t(\log n)$ except for configuration 1^n				
132 (222)	FG	0^n (unreachable), 1^n (unreachable), $(01)^n$, $(CA^i BE(DE)^j)^k$	-				
134 (148, 158, 214)	BFG	0^n (unreachable), 1^n (unreachable), $(01)^n$	To a non-trivial configuration with probability p				Very close to coalescence
136 (192, 238, 252)	EG	0^n , 1^n (unreachable)	Trivial in $t(\log n)$ except for configuration 1^n				
138 (208, 174, 244)	BEG	0^n , 1^n (unreachable)	Trivial in $t(n^2)$ except for configuration 1^n				

Wolfram's code	Fatès' code	Fixed points	Coalescence style	Space-time diagram I	Space-time diagram II	Agreement space-time diagram of I and II	Comments
140 (196, 206, 220)	G	0^n (unreachable), 1^n (unreachable), $(01)^n$, $(CA^i BE(DE)^j)^k$	-				
142 (212)	BG	0^n (unreachable), 1^n (unreachable), $(01)^n$	To a non-trivial configuration with probability p				Very close to coalescence or full disagreement
146 (182)	BCEFG	0^n , 1^n (unreachable)	Trivial in $t(n^2)$ except for configuration 1^n				
150	BCFG	0^n (unreachable), 1^n (unreachable), $(01)^n$	-				
152 (194, 230, 188)	CEG	0^n , 1^n (unreachable)	Trivial in $t(n^2)$ except for configuration 1^n				
154 (210, 166, 180)	BCEG	0^n , 1^n (unreachable)	To a non-trivial configuration in $t(n^2)$				Coalesces a long time before reaching the fixed point
156 (198)	CG	0^n (unreachable), 1^n (unreachable), $(01)^n$	-				
160 (250)	DEFG	$0^n, 1^n$	With probability p				Could be trivial in $t(\log n)$ for a subset of configurations
162 (176, 186, 242)	BDEFG	$0^n, 1^n$	With probability p				Could be trivial in $t(\log n)$ for a subset of configurations
164 (218)	DFG	0^n (unreachable), 1^n , $(CA^i BE)^j$	-				
168 (224, 234, 248)	DEG	$0^n, 1^n$	With probability p				Could be trivial in $t(\log n)$ for a subset of configurations
170 (240)	BDEG	$0^n, 1^n$	With probability p				May coalesce before reaching the fixed point

Wolfram's code	Fatès' code	Fixed points	Coalescence style	Space-time diagram I	Space-time diagram II	Agreement space-time diagram of I and II	Comments
172 (228, 202, 216)	DG	0^n (unreachable), 1^n , $(CA^i BE)^j$	-				
178	BCDEFG	$0^n, 1^n$	With probability p				
184 (226)	CDEG	$0^n, 1^n$	With probability p				
200 (236)	E	0^n , 1^n (unreachable), $(CA^i BFH^j G(DFH^k G)^l)^m$					
204	I	All configurations	-				
232	DE	$0^n, 1^n$, $(CA^i BFH^j G)^k$	-				